

UNCLASSIFIED

AD 4 2 3 9 3 8

DEFENSE DOCUMENTATION CENTER

FOR

SCIENTIFIC AND TECHNICAL INFORMATION

CAMERON STATION, ALEXANDRIA, VIRGINIA



UNCLASSIFIED

NOTICE: When government or other drawings, specifications or other data are used for any purpose other than in connection with a definitely related government procurement operation, the U. S. Government thereby incurs no responsibility, nor any obligation whatsoever; and the fact that the Government may have formulated, furnished, or in any way supplied the said drawings, specifications, or other data is not to be regarded by implication or otherwise as in any manner licensing the holder or any other person or corporation, or conveying any rights or permission to manufacture, use or sell any patented invention that may in any way be related thereto.

423938

TURBULENT DISPERSION IN A PIPE FLOW

H. A. Becker
R. E. Rosensweig
J. R. Gwozdz

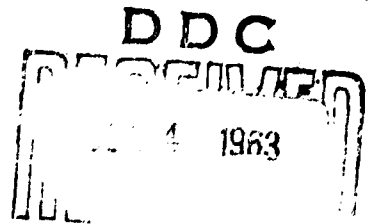
Fuels Research Laboratory
Massachusetts Institute of Technology
Cambridge 39, Massachusetts

Contract No. AF19(604)-6181
Project No. 8604
Task 86040

FINAL REPORT
September, 1963

Prepared
for

AIR FORCE CAMBRIDGE RESEARCH LABORATORIES
OFFICE OF AEROSPACE RESEARCH
UNITED STATES AIR FORCE
BEDFORD, MASSACHUSETTS



Requests for additional copies by Agencies of the
Department of Defense, their contractors, and other government
agencies should be directed to

DEFENSE DOCUMENTATION CENTER (DDC)
CAMERON STATION
ALEXANDRIA, VIRGINIA

FOREWORD

The contract under which the work herein reported was done was first held by Professor C. C. Lin of the Department of Mathematics of Massachusetts Institute of Technology, who conducted a theoretical study of turbulent dispersion. Towards the close of Professor Lin's contract period, Professor R. E. Rosensweig of the Institute's Department of Chemical Engineering proposed a contractual extension to facilitate an experimental study of some of the questions raised by Lin. When Rosensweig left to join the AVCO Corporation, the work was undertaken, at his invitation, by his colleague, Professor H. A. Becker.

The work reported herein was conducted in the Fuels Research Laboratory of the Chemical Engineering Department of Massachusetts Institute of Technology. This Laboratory is engaged chiefly in the study of combustion phenomena, and in these turbulent diffusion is often a leading actor. The kindness of the Laboratory's Directors, Professors H. C. Hottel and G. C. Williams, in opening their facility to the present investigation is gratefully acknowledged.

Messrs. C. Crawford and J. R. Gwozdz, Master of Science students in the Department of Chemical Engineering, served as Research Assistants. Mr. Crawford assisted with the construction of the apparatus. Mr. Gwozdz, while taking the greater part of the data, showed such integrity and perseverance in his work that he has been accounted a co-author of the investigation's result.

Dr. Rosensweig is presently a member of the Research and Advanced Development Division of AVCO, at Wilmington, Massachusetts. Professor Becker is on the faculty of the Department of Chemical Engineering of Queen's University, at Kingston, Ontario. Mr. Gwozdz is continuing his studies at M.I.T.

ABSTRACT

Turbulent diffusion from a point source in a pipe flow has been studied. It was desired to verify Richardson's law and to evaluate the parameter B in Lin's derivation of that law. Difficulties were encountered and the data obtained were insufficient for these purposes. A very considerable quantity of novel and useful information was nevertheless gathered. The scattered-light technique was used to map the fields of point-concentration fluctuations and of the mean concentration in the diffusion plume. The relative intensity of the point-concentration fluctuations was found to be of the order of 100% on the plume axis and increased towards the plume edges. The parameters in Taylor's theory were evaluated; the intensity of fluctuations in the radial component of the velocity of a diffusing particle was estimated to be 2.84% of the centerline velocity in the pipe, and the Lagrangian (spatial) integral scale was found to be of the magnitude of 8.3% of the pipe radius. The value resulting for the turbulent Peclet number (the product of pipe diameter times centerline velocity divided by turbulent diffusivity) is 852. The use of sheet-illumination in the scattered-light technique facilitated the measurement of fluctuations in the integral concentration of material in a plume cross-section. The relative intensity of these fluctuations was of the order of 30%. Spectral analyses were made of both point- and sheet- concentration fluctuations and integral turbulence scales were estimated from the data.

CONTENTS

	<u>PAGE</u>
INTRODUCTION	1
THE TURBULENCE FIELD	3
THE SCATTERED-LIGHT TECHNIQUE	4
THE APPARATUS	
The pipe	6
Ancillary ducting	6
Fog injectors	7
Oilfog generator	9
Lighting optics	9
Phototransducer	9
INSTRUMENTATION AND METHODS OF MEASUREMENT	
Velocity and flowrate	13
Electrical measurements	13
SOURCES OF ERROR	14
RESULTS	
Pipeflow parameters	15
The field of the mean point-concentration	15
The spectrum of point-concentration fluctuations	26
The intensity of point-concentration fluctuations	29
The intensity of sheet-concentration fluctuations	33
The spectrum of sheet-concentration fluctuations	35
Meandering	44
DISCUSSION	49
REFERENCES	52

FIGURES

1 Oilfog injector "A" in position on the test pipe . . .	10
2 Light source and beam-defining optics for point-concentration measurements	11
3 Light source and beam-defining optics for sheet-concentration measurements	12
4 Normalized radial profiles of the point concentration	17
5 Normalized radial profiles of the point concentration	18
6 The concentration half-radius of the plume as a function of distance from the source	22
7 The square of the concentration half-radius as a function of distance from the source	23

8	Normalized spectra of point concentration fluctuations	27
9	Normalized radial profiles of the intensity of point-concentration fluctuations	30
10	Normalized radial profiles of the relative intensity of point-concentration fluctuations	31
11	Normalized radial profiles of the relative intensity of point-concentration fluctuations	32
12	The normalized intensity of sheet-concentration fluctuations as a function of distance from the source	36
13	A representative spectrum of sheet-concentration fluctuations	37
14	Spectra of sheet-concentration fluctuations at various distances from the source	38
15	Spectra of sheet-concentration fluctuations near the source at various flow velocities	40
16	Spectra of sheet-concentration fluctuations far from the source at various flow velocities	41
17	Relation between the centroid of the spectrum of sheet-concentration fluctuations and distance from the source	42
18	Relation between the maximum-point of the spectrum of sheet-concentration fluctuations and distance from the source	43
19	Transducer location for the detection of meandering	46

PLATES

1	View of the apparatus on the roof of the Fuels Research Laboratory, Massachusetts Institute of Technology . .	8
---	---	---

TABLES

1	Flow parameters calculated from the centerline velocity and the frictional pressure drop	15
2	Constancy of the product $\bar{\Gamma}_c r_{1/2}^2$ at $Re_p = 684,000$. .	25

NOTATION

The instantaneous values of statistically-steady turbulently fluctuating quantities are in this report denoted by capital letters. The time-mean value (indicated by an overbar) of such a quantity W is

$$\bar{W} \equiv \lim_{T \rightarrow \infty} \frac{1}{T} \int_t^{t+T} W \, dt.$$

The fluctuations of such quantities are denoted by lower-case letters, e.g., $w \equiv W - \bar{W}$. The mean-square amplitude of a fluctuation w is

$$\overline{w^2} \equiv \lim_{T \rightarrow \infty} \frac{1}{T} \int_t^{t+T} w^2 \, dt,$$

The root-mean-square amplitude (indicated by the oversign \wedge) follows as $\hat{w} \equiv \sqrt{\overline{w^2}}$. The root-mean-square amplitude of fluctuation is commonly called the intensity of fluctuation.

Coordinates:

- x, r, ρ cylindrical coordinates (with x along the plume or pipe axis, originating at the plume source, and positive in the downstream direction)
 x, y, z Cartesian coordinates (with x as in cylindrical coordinates)
 t time

Subscripts:

- c centerline value
 m maximum

Variables:

- B Lin's turbulence parameter
 C correlation coefficient for point-concentration fluctuations at two points in space
 D_p pipe diameter
 \mathcal{D}_M molecular diffusivity

\mathcal{D}_T	turbulent diffusivity
$E_{Y1}(k_1)$	spectral density function for point-concentration fluctuations
f	frequency
J	source strength (source material flux)
k_1	wave number ($\equiv 2\pi f / \bar{U}$)
K	correlation coefficient for sheet-concentration fluctuations occurring in two plume cross-sections
L	distance from pipe axis to photo-transducer at side of pipe
P	mean-square relative fluctuation sensed by a phototransducer viewing a plume cross-section edgewise
Pe_T	turbulent Peclet number ($\equiv D_p \bar{U}_c / \mathcal{D}_T$)
Q	correlation coefficient for the signals produced by two phototransducers viewing a plume cross-section edgewise from opposite sides of the plume
r_p	pipe radius
$r_{1/2}$	concentration half-radius of plume
\bar{r}^2	mean-square material displacement radius of plume
Re_p	pipe Reynolds number ($\equiv D_p U_{av} \rho / \mu$)
S	sensitivity of phototransducer
U	axial (x-) component of velocity
U_{av}	average flow velocity through pipe (discharge divided by area)
v	radial component of turbulent velocity fluctuation
$W(k_1)$	spectral density function for sheet-concentration fluctuations
\bar{y}^2	mean-square y- component of material displacement from the time-mean center of gravity ($\bar{y}^2 = 1/2 \bar{r}^2$ here)
Y^2	mean-square y- component of material displacement from the instantaneous center of gravity
\bar{Y}_0^2	mean-square y- component of the displacement of the instantaneous center of gravity from the time-mean center
Γ	point-concentration
γ	point-concentration fluctuation
ζ, η, ξ	distance of separation between pairs of points in space
Λ_L	Lagrangian scale of turbulence
Λ_γ	integral spatial scale of point-concentration fluctuations
Λ_w	integral spatial scale of sheet-concentration fluctuations

μ	viscosity
ρ	density
Ω	sheet-concentration
w	sheet-concentration fluctuation

INTRODUCTION

The turbulent dispersion of matter released from a point source can be described (6, 9) by the superposition of two processes: Firstly, turbulent motions small in spatial scale relative to the material cloud cause the material to spread about the instantaneous center of gravity. Secondly, large-scale turbulent motions cause meandering (aimless wandering) of the instantaneous center of gravity. In small dispersion times t , dispersion is due mostly to meandering, and Taylor's theory of single-particle diffusion (21) predicts that the mean-square displacement, \bar{y}^2 , of material from the time-mean center of gravity is proportional to the square of the dispersion time, t^2 . For dispersion effected by turbulence concentrated within an equilibrium convection subrange, the similarity theory of turbulent dispersion predicts that the mean-square displacement, \bar{Y}^2 , from the instantaneous center of gravity is proportional to the cube of the dispersion time, t^3 , a relation first suggested by Richardson (17) and known after him as Richardson's law. Lin (15) has recently derived Richardson's law from a kinematic analysis of two-particle turbulent dispersion. It is, of course, physically necessary that \bar{y}^2 and \bar{Y}^2 eventually converge to a limiting ratio. For large dispersion times, both \bar{y}^2 and \bar{Y}^2 are expected to, and Taylor's theory predicts that \bar{y}^2 will, vary linearly with time: \bar{y}^2 or $\bar{Y}^2 \propto t - t_0$ (t_0 is the virtual temporal origin of the final period).

The predictions of Taylor's theory have been amply confirmed by experiment (10). Studies of oceanic (20) and atmospheric (11) turbulent dispersion have indicated the validity of Richardson's law, but measurements under well-controlled conditions are lacking.

The statistical theories of Taylor and Lin result in predictions for the mean concentration field in a turbulent diffusion plume but cast no light on the turbulent concentration fluctuations. The fluctuating plume model of Gifford (9) attempts to predict concentration fluctuations by attributing these to the meandering of an otherwise stationary concentration pattern. This is certainly but a partial approximation to reality, and what the model neglects may be more important than the effect it accounts for. Gifford's basic assumption must be experimentally validated before his theory can be accepted; i.e., it must be demonstrated that meandering is a sufficiently large effect to alone account for the bulk of the concentration fluctuation occurring at a point.

Published data on concentration fluctuation in gaseous systems are fragmentary. The best available are those of Corrsin and Uberoi (7), who made measurements at a few points downstream of a line source of heat in a turbulent jet of air. Lee and Brodsky (14) recently studied concentration fluctuation in a pipe flow of water, using a dye solution injected from a point to generate a turbulent diffusion plume (the measurements were made with an optical probe, utilizing light absorption by the dye).

Recently Rosensweig (18, 19) developed a scattered-light technique for studying the concentration field of suspended colloidal particles marking one of the fluid streams entering a mixing field. A linear response is obtained to both the time-mean and the time-variant components of material concentration at a point, in a sheet, or in a volume, according to the modes of illumination and observation. In particular, turbulent concentration fluctuations can be accurately detected and electronically analysed. Rosensweig investigated turbulent mixing between a free jet of air (marked by an oilfog) and the clear ambient air. Becker (3, 4, 5) subsequently refined the technique and studied jet-mixing in a confined-jet system.

It was clear, on considering systems for further exploitation of the scattered-light technique, that turbulent dispersion is a most basic mixing problem and that a thorough investigation would yield a wealth of novel, useful, and fundamentally significant information. A theoretical study of turbulent dispersion had been proceeding in the Mathematics Department of Massachusetts Institute of Technology under Professor Lin and under the present sponsorship. It was therefore proposed to modify the terms of the contract to facilitate the present experimental investigation. The primary objects were to be (a) to verify Richardson's law, and (b) to investigate as a function of Reynold's number the relationship between the rate of dissipation of turbulent energy and the parameter B occurring in Lin's derivation of Richardson's law. It was further proposed to measure point-concentration fluctuations in a turbulent diffusion plume and also the fluctuations in integral material content over a cross-section of the plume. Appropriate measurements on a cross-section would indicate meandering and permit a test of Gifford's theory.

The nearly homogeneous, isotropic turbulence field in the core of a fully developed pipe flow was chosen as the vehicle for turbulent

dispersion. A 20 cm diameter aluminum irrigation pipe, 90 pipe diameters long, was used. A point source for turbulent diffusion was approximated by a hypodermic tubing injector from which there issued, at the local mean flow velocity in the pipe, a steady stream of oilfog.

It was hoped, at first, to study Richardson dispersion directly by the technique of photographing "instantaneous" views of cross-sections of the diffusion plume by sheet flash illumination and then analysing the negatives on a densitometer (there appears to be no feasible method by which a signal can be formed which measures in situ the mean-square displacement of material from the instantaneous center of gravity of a cross-section of a diffusion plume). It was soon apparent that the required photographic work could not be done within the time and with the personnel available. The direct measurement of Richardson dispersion was therefore abandoned and attention was focused on the other lines of investigation.

The fields of the mean and r.m.s. fluctuating point-concentration were mapped at several Reynolds numbers over a distance of six pipe diameters downstream of the source. Spectral analyses were made of the point-concentration fluctuations at several points on the plume axis. With the use of sheet illumination, measurements were made of the mean and fluctuating components of the integral material concentration in a plume cross-section and the fluctuating component was spectrally analysed. A method was devised for detecting meandering, using sheet illumination, but no measurable meandering could be observed. Evidently meandering is a small effect within the regimes studied. Meaningful measurements could not be made very near the source (where meandering is the dominant mode of dispersion), owing to the disturbance of the pipe flow by the injector.

THE TURBULENCE FIELD

It would be desirable, in order to most clearly define the problem and reduce it to its basic essentials, to study turbulent

dispersion in a field of homogeneous, isotropic turbulence. While such a field is not practically realizable, it is approximated in two situations: (i) some distance downstream of a turbulence-generating grid in a statistically uniform flow, and (ii) the core of a well-established turbulent pipe flow. The latter system was chosen for this investigation because (i) it is simpler to install in the laboratory, (ii) a non-arbitrary design condition exists (i.e., fully developed turbulent flow through a smooth, round pipe), (iii) for this easily realized standard condition, there is an extensive literature on the fields of the mean and fluctuating components of velocity (10, 12) and on the field of mean concentration downstream of a point source (1, 8, 10, 22), (iv) the core of a pipe flow is a region of nearly homogeneous, isotropic turbulence; the spatial components of velocity fluctuation are nearly equal, along the axis the shear stress is zero, and there is strict homogeneity in the mean flow direction, and (v) pipe flow is of considerable practical importance.

THE SCATTERED-LIGHT TECHNIQUE

The scattered-light technique is a technique for studying material mixing between several streams by marking one of these with a sol (a suspension of colloidal particles) and using the light-scattering property of the sol to detect the material of the marked stream. The principle of the technique is simple: The zone of a mixing field within which it is desired to detect the quantity of the marking sol is uniformly illuminated and light scattered from the volume of interest (usually at right-angles to the incident beam) is focused on a photocell. The photocell gives an electrical signal linear in the instantaneous content of sol, M , assuming, as is normally true, that the characteristics of the sol particles are invariant over the field.

$$M = \int_V \Gamma \, dV,$$

where Γ is the point-concentration of sol and V is the volume of interest. The electrical signal is then analysed electronically; e.g., a d.c. voltmeter gives the time-mean material content \bar{M} ,

$$\bar{M} = \lim_{T \rightarrow \infty} \frac{1}{T} \int_t^{t+T} M \, dt.$$

The detection of point-concentrations requires the use of a small-diameter beam of light. A lens viewing the beam at right angles focuses the scattered light on a slitted diaphragm, forming thereon an image of the incident beam. The slit passes the light scattered from a short segment of the incident beam to a photocell. That segment then defines the volume observed. When the observed volume is sufficiently small, the photocell signal is directly proportional to the instantaneous point concentration, i.e.,

$$\lim_{V \rightarrow 0} \int_V \Gamma \, dV = \Gamma V.$$

The criteria for sufficient smallness of the observed volume are now well known (5, 18).

Measurement of the material concentration in a cross-section of a flow,

$$\Omega \equiv \int_A \Gamma \, dA$$

where A is the area viewed, requires the use of an uniform sheet of light. At a distance from the sheet-illuminated mixing zone sufficiently great so that differences in optical path length are effectively negligible, scattered light is gathered by a lens and focused on a photocell. When the observed layer is thin enough, the signal is directly proportional to Ω .

THE APPARATUS

The Pipe

The experimental realization of a fully developed pipe turbulence requires (a) a very long pipe, and (b) a very high pipe Reynold's number. It was decided that a pipe approximately 20 cm in diameter by 100 diameters long and an average air flow velocity of about 50 m/sec (giving a Reynold's number of 700,000) would satisfy these conditions as closely as possible within the scale of operation feasible in the laboratory.

The pipe installed was a 90 diameter-long straight run of 8-inch nominal diameter aluminum irrigation piping. The true inside diameter was 20.1 cm, based on the inside circumference. Straightening vanes and calming screens were provided at the inlet. The 90-diameter length was judged sufficient for a very close approach to equilibrium flow over the final six diameters of length which constituted the test section.

In operation, longitudinal traverses of the diffusion plume were made by observing a fixed cross-section of the flow and varying the position of the oilfog injector, and not vice-versa. To ease the problem of optical observation, the cross-section of interest was located, not inside the pipe, but 5 cm beyond its end; experience with jets showed that the core flow pattern would suffer no measurable change over this short distance. The pipe was tapped for insertion of the oilfog injector at intervals of 5.1 cm (2 inches) over the final six diameters of length.

Ancillary Ducting

There was no interior building space available for the installation of a 20 m straight run of pipe and so the apparatus was set up on the roof of the Fuels Research Laboratory of the Department of Chemical Engineering, open to sun and weather. It was therefore necessary to provide a light-tight housing for the light-scatter apparatus and to assure complete darkening of the test section. To this end, the test pipe was connected to

a 10 m straight run of 30 cm (12 inch) diameter galvanized furnace ducting painted flat black on the inside and terminating in a 45° downbend. The first section of the furnace pipe was a tee and the phototransducers were housed in sections of pipe connected to the arms of this tee. The sudden enlargement in the main run of ducting on entering the furnace pipe was sufficient to carry the discharge from the test section past the tee before recontacting the duct wall, and at no time was any oilfog observed to recirculate past or enter into the phototransducer chambers. With this arrangement, the test section at the exit of the test pipe was in effect totally light-tight, i.e., no light leaks could be detected above the thermal noise level of the phototubes. The furnace pipe enclosing the test section was lined with black velveteen cloth to reduce the reflectivity to a negligible value. The external appearance of the final installation is seen in Plate 1.

Fog Injectors

Two fog injectors were made of 12-gauge hypodermic tubing (2.77 mm O.D., 2.16 mm I.D.). Oilfog was injected at the local mean velocity of the pipe flow. Ideally such an injector should be vanishingly small, in order not to perturb the flow. In practice, however, the injector had to provide a sufficiently copious flow of fog to raise fog concentrations in the diffusion plume to a level high enough for proper use of the scattered-light technique.

Injector A was designed for the injection of fog on the axis of the pipe and was streamlined for minimum disturbance of the flow. Injector B was built later, when it was undertaken to make radial traverses of the diffusion plume. It would have been expensive in arrangement and clumsy of execution to traverse the flow radially with the light-scatter equipment. The much simpler alternative of moving the fog injector across the diameter of the flow and holding the point of observation fixed on the axis was therefore chosen and injector B was designed

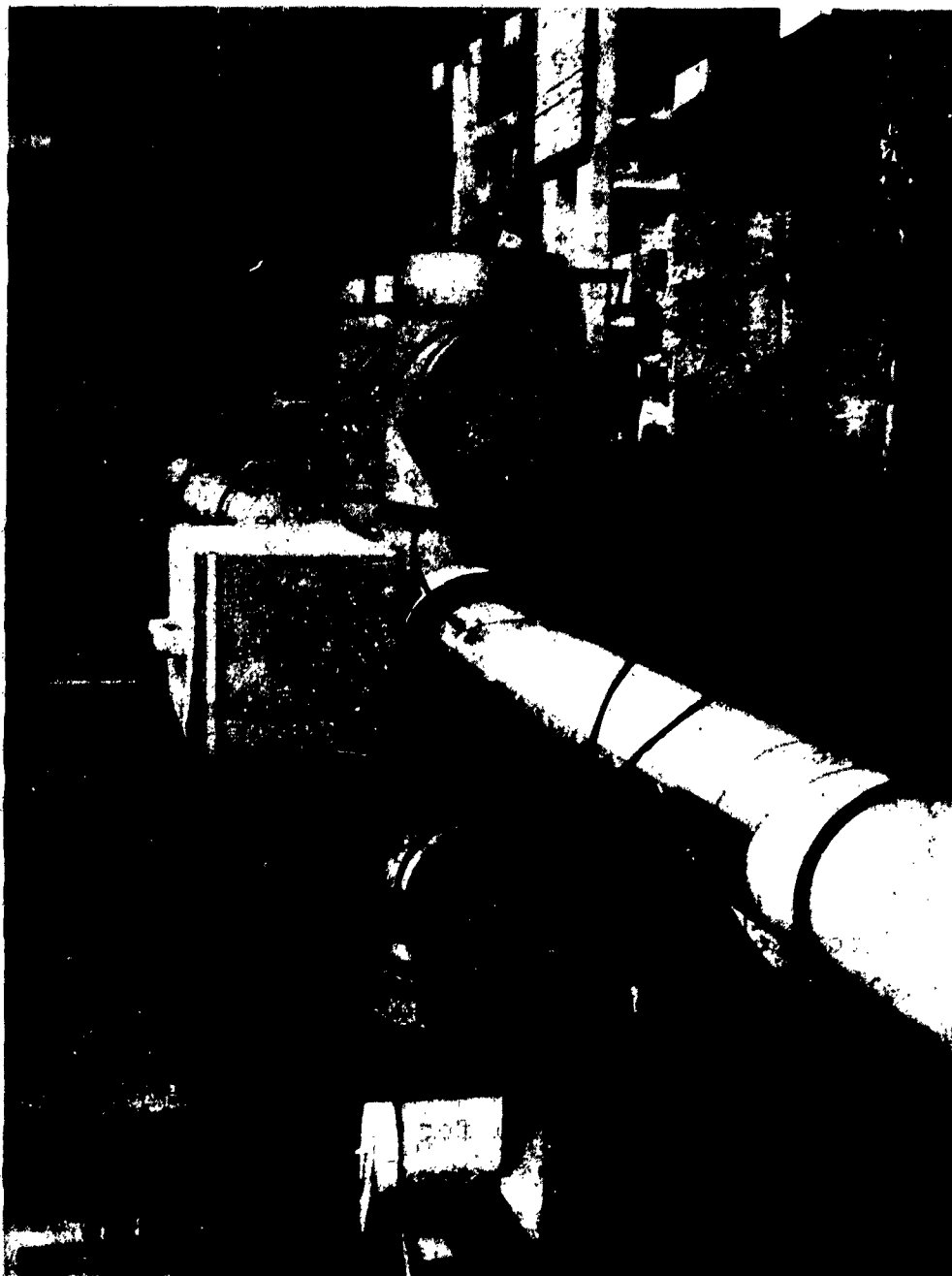


Plate 1: VIEW OF THE APPARATUS ON THE ROOF OF THE
FUELS RESEARCH LABORATORY, MASSACHUSETTS
INSTITUTE OF TECHNOLOGY

for this purpose. Because of the pressure of time, this injector was made very simply, omitting such desirable refinements as streamlining and micrometer positioning.

The method of mounting the injectors in the pipe is shown in Fig. 1, which shows injector A in position.

Oilfog Generator

The oilfog generator described by Becker (3) was used. In this generator, a hydrocarbon oil (sold by Esso under the name "Coray 55") of narrow molecular weight range and with an average molecular weight of about 300 is evaporated into a hot stream of air. The air-vapor mixture is then rapidly cooled, forming the oilfog.

Lighting Optics

A 100-watt concentrated-arc (zirconium arc) lamp was used as a light source. For point-concentration measurements, a narrow beam of light was produced by the optical system shown schematically in Fig. 2. Light from the lamp was collected by two simple convex lenses and focused on a diaphragm. Light passing through the circular diaphragm aperture was collected by a pair of projection lenses and focused on a spot in the field under study. The diameter of the lightbeam at the point of focus was controlled by the size of the aperture.

For sheet-concentration measurements, a sheet of light adequately uniform in thickness and intensity was produced by the arrangement shown in Fig. 3.

Phototransducer

The phototransducer for the light-scatter measurements consisted of a chassis box containing an RCA 931A multiplier phototube and its associated circuitry and having attached to it a barrel containing a lens for gathering scattered light. In the case of point-concentration measurements, the light gathered was focused on a slitted diaphragm, forming an image of the incident beam. The diaphragm actually consisted of

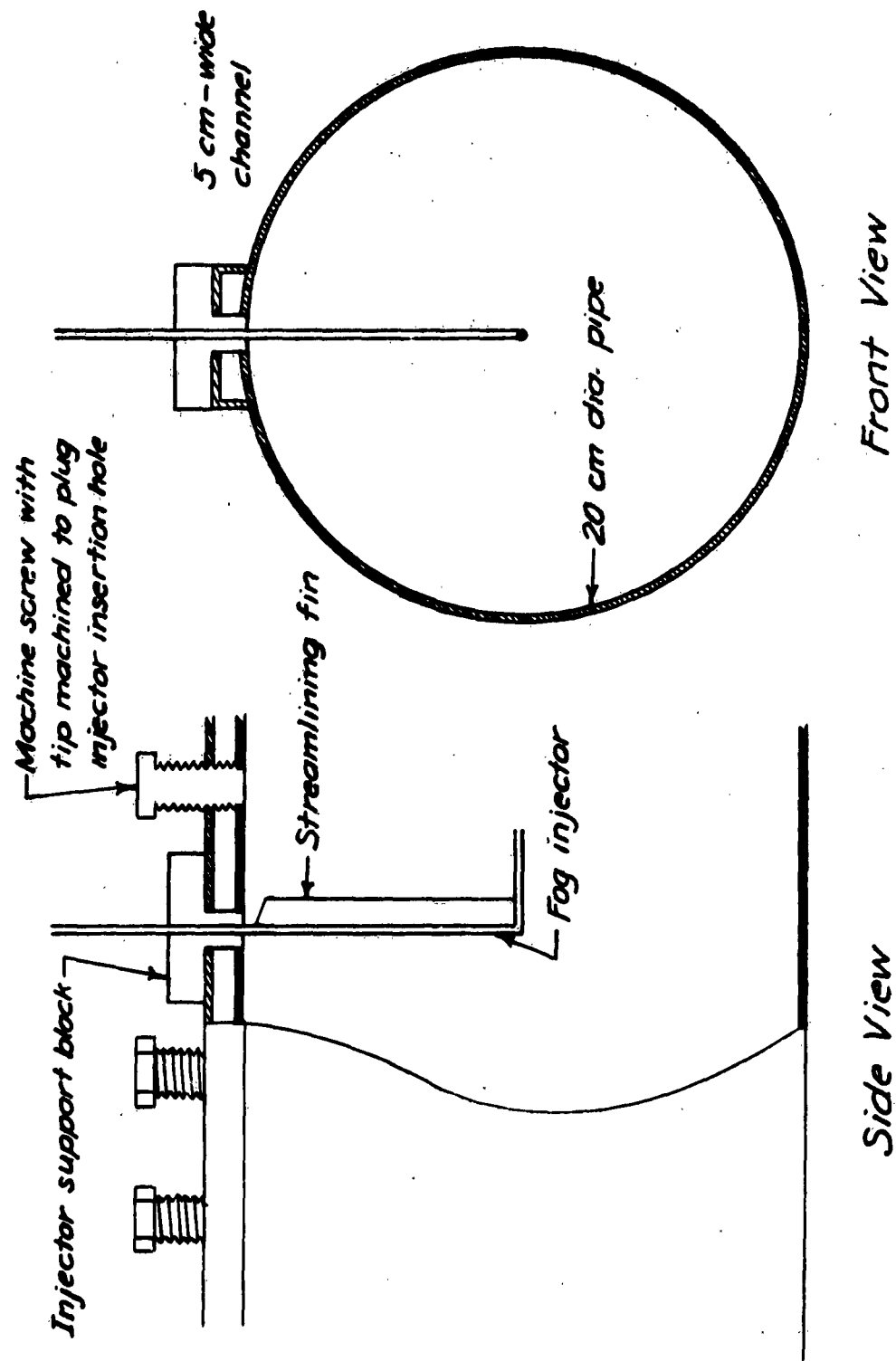


Figure 1: OILFOG INJECTOR 'A' IN POSITION ON THE TEST PIPE

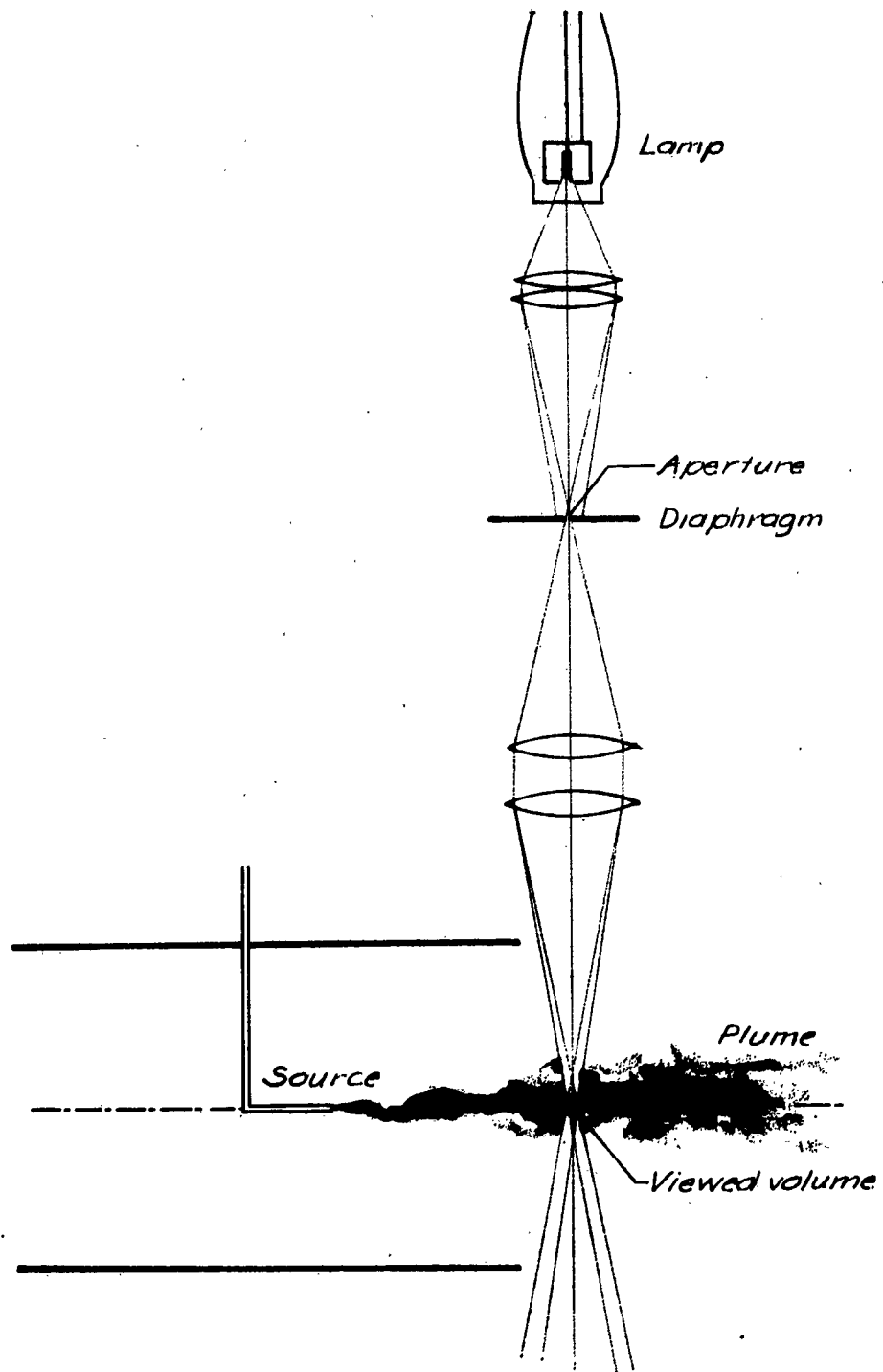


Figure 2: LIGHT SOURCE AND BEAM DEFINING OPTICS FOR POINT-CONCENTRATION MEASUREMENTS.

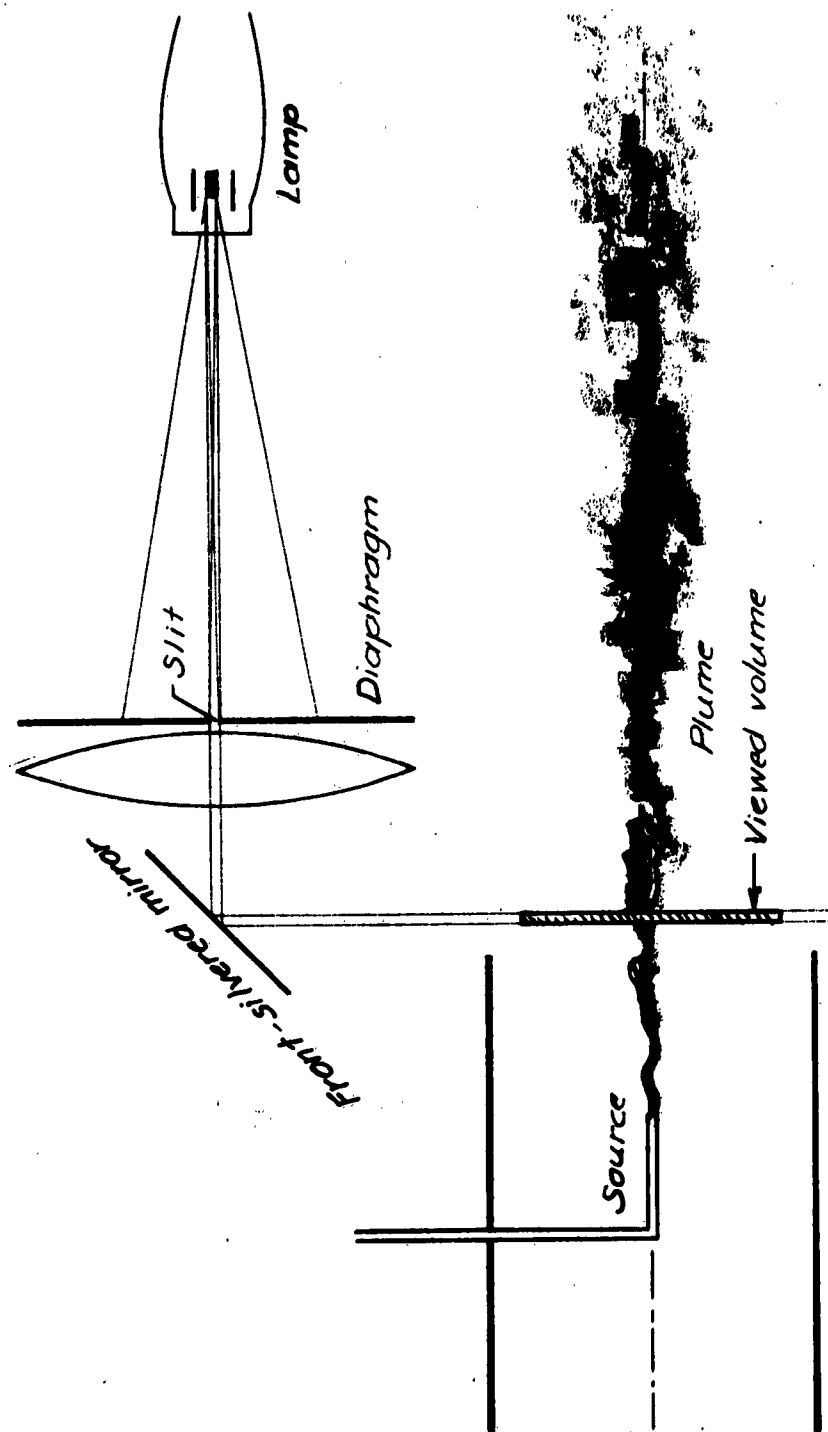


Figure 3: LIGHT SOURCE AND BEAM-DEFINING OPTICS FOR SHEET-CONCENTRATION MEASUREMENTS

tape stuck onto the glass jacket of the phototube. The slit passed to the phototube light scattered from a short segment of the focal region of the incident beam. In the case of sheet-concentration measurements, the lens was arranged with the photocathode of the phototube at its principal focus. The transducer was then positioned with the lens at a distance of 20 - 40 cm from the test-pipe axis. Light scattered from the sheet-illuminated cross-section of the diffusion plume and gathered by the viewing lens then fell on a small, essentially stationary spot on the photocathode.

INSTRUMENTATION AND METHODS OF MEASUREMENT

Velocity and Flowrate

The mean velocity on the pipe axis was measured with a Pitot tube. The frictional pressure drop was measured between static pressure taps 543 cm apart. The volumetric-mean velocity of discharge (U_{av}) was then deduced from its standard relation with the pipe friction factor and the centerline velocity, using the correlations given by Hinze (10).

The oilfog flow rate was measured with a standard square-edged orifice.

Electrical Measurements

The electrical signal from the phototube (or tubes) was processed with the following instruments: a d.c. voltmeter accurate to $\pm 1\%$; a true r.m.s. voltmeter accurate to $\pm 1/2\%$; a sound analyser accurate to $\pm 2\%$ in frequency setting and calibrated with white noise as to amplitude response; and a correlation amplifier for measuring correlation coefficients with an accuracy of ± 0.01 . A number of lowpass filters were used to rid the signal of random noise contained in frequencies above the range of significant turbulence-energy content.

SOURCES OF ERROR

The only source of error worthy of a detailed examination is the disturbance of the pipe flow by the fog injectors,

The pressure drop occasioned by the streamlined injector A was not detectable. The non-streamlined injector B was equal in effect (when centered on the pipe axis) to a half-diameter length of pipe. The turbulence generated by injector B can be roughly characterized: The mean-square maximum velocity fluctuation downstream of an infinite cylinder in an uniform stream is approximately $\overline{u^2} = 0.07 U^2 D_{cyl}/x$, where D_{cyl} is the cylinder diameter. At a distance of 100 cylinder diameters, the fluctuation is of about the same intensity as in the core of a pipe flow, $\overline{u^2} \approx 0.0001 \overline{U^2}$. At 200 cylinder diameters, $\overline{u^2}/U^2$ is about 1/4 as high as in a pipe. In the present system, 100 cylinder diameters were equivalent to 1 1/2 pipe diameters.

As a result of the disturbances generated by injector B, the fields of the mean point-concentration and the point-concentration fluctuation intensity were somewhat distorted at the fringes of the diffusion plume, but not in the core. The data taken over the half of a diametrical traverse in which the injection point was between the pipe axis and the point of insertion of the injector through the pipe wall were therefore taken as definitive, since the point of measurement was then least disturbed. The point of measurement was, as noted earlier, fixed on the pipe axis.

The disturbing effect of the injector could be large only very near the source. The present measurements were begun at a distance of about 3 pipe diameters from the source. The differences between the actual data at this distance and those that would have been obtained with a truly passive source are probably measurable but not serious.

RESULTS

Pipeflow Parameters

Measurements of the frictional pressure drop were made at pipe Reynolds numbers $Re_p \equiv D_p U_{av} \rho / \mu$ of 481000 and 684000. The resulting values for the average velocity of discharge U_{av} , the friction factor $f \equiv D_p (dp/dx) / (1/2 \rho U_{av}^2)$, and the "friction velocity" $u^* \equiv \sqrt{\tau_o / \rho}$ are summarized below in Table 1. The pressure drops were about 10% higher than would occur in a perfectly smooth pipe, and the friction factors indicate a relative pipe roughness of 0.00007.

TABLE 1
FLOW PARAMETERS CALCULATED FROM THE CENTERLINE VELOCITY
AND THE FRICTIONAL PRESSURE DROP

Re_p	f	U_{av} / \bar{U}_c	u^* / \bar{U}_c
481,000	0.01397	0.8567	0.186
684,000	0.01357	0.8587	0.184

The Field of the Mean Point-concentration

The field of the mean point-concentration of material in a diffusion plume generated by a point source in the core of a pipe flow has been studied by numerous investigators (1, 8, 10, 16, 22). The present data may be better than any previously obtained, owing to the directness and simplicity of the scattered-light technique: The light probe does not perturb the flow and the measurements are made in situ (i.e., material does not have to be withdrawn for analysis). Moreover, traverses are made easily and quickly and so the effects of any gradual drift in operating conditions are minimal.

The field of the mean point-concentration, \bar{F} , was studied at several pipe Reynolds numbers, the highest being 684000.

This maximum Reynolds number is about 10% higher than has previously been realized in such experiments and, according to the data compiled by Hanratty, Kada, and Flint (8), is certainly high enough to assure location within the regime of Reynolds number independence of the turbulent material diffusivity.

The radial concentration profile in a diffusion plume is normally bell-shaped and is characterizable as to scale by two amplitudes; (1) the central maximum of the concentration, \bar{F}_0 , and the radius, $r_{1/2}$, at which the concentration is one-half the maximum,

$$r = r_{1/2} \text{ at } \bar{F} = 1/2 \bar{F}_0.$$

In the presence of self-preservation (i.e., invariance under downstream translation), \bar{F}/\bar{F}_0 is a unique function of $r/r_{1/2}$:

$$\bar{F} = \bar{F}_0 \cdot g(r/r_{1/2}).$$

More generally, however, the distribution function g depends on the distance from the source. At small values thereof, g is also a function of the pipe Reynolds number.

Figure 4 shows a normalized representation of the data for the highest Reynolds number, 684,000. To the accuracy of the data, the radial concentration profile is self-preserving up to $r = r_{1/2}$. Beyond this point, the profile becomes narrower-skirted with increasing distance from the source. The data for large radii are better seen in a semilogarithmic presentation, Figure 5. The self-preserving core is exactly described by the normal distribution function

$$\bar{F} = \bar{F}_0 \exp(-0.693 r^2/r_{1/2}^2), \quad r < r_{1/2} \quad (1)$$

At larger radii the data diverge and no limiting form appears to be approached either near to or far from the source. In the case of a truly homogeneous, isotropic field of turbulence translated past the point of observation at a uniform velocity,

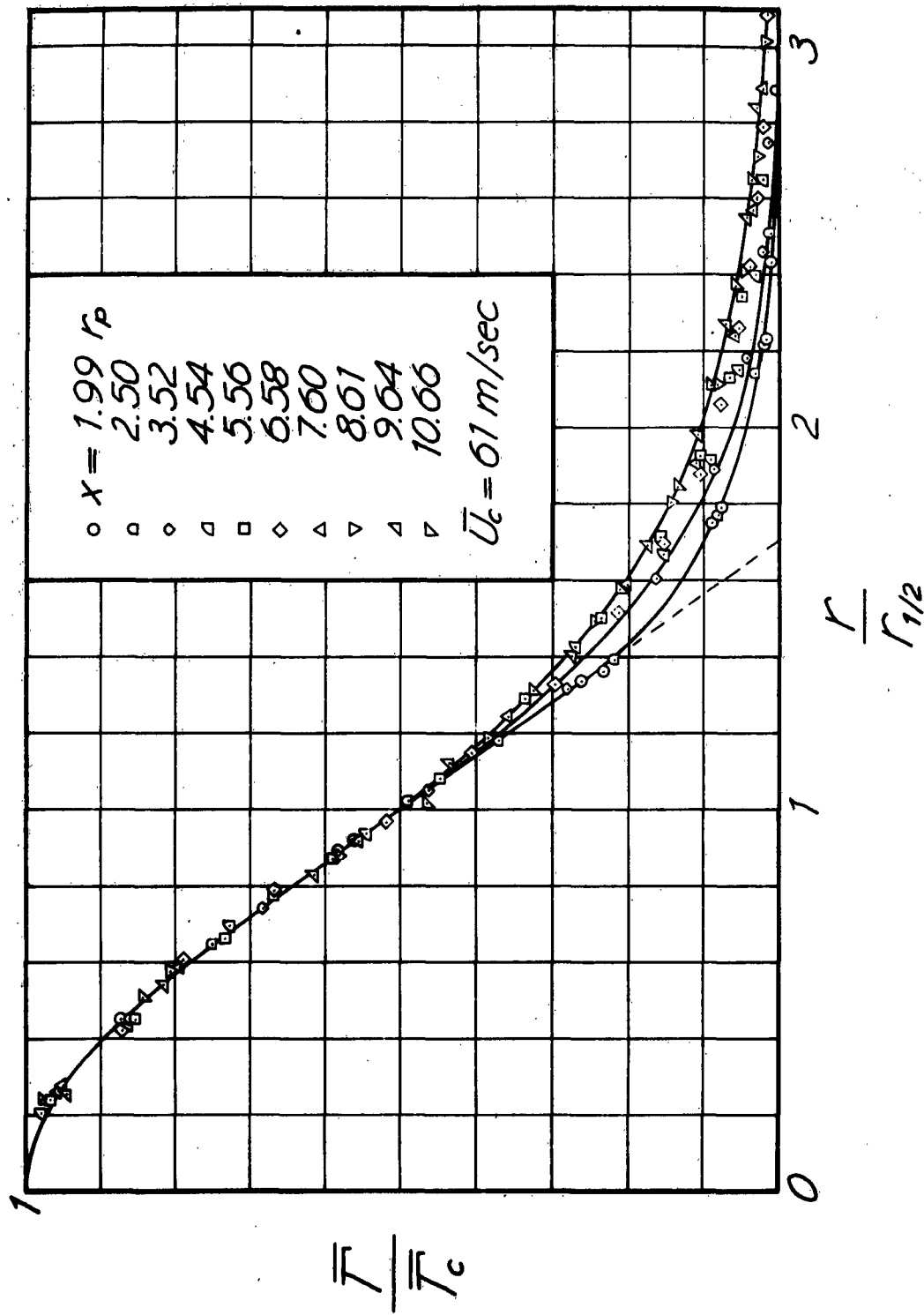


Figure 4: NORMALIZED RADIAL PROFILES OF THE POINT CONCENTRATION

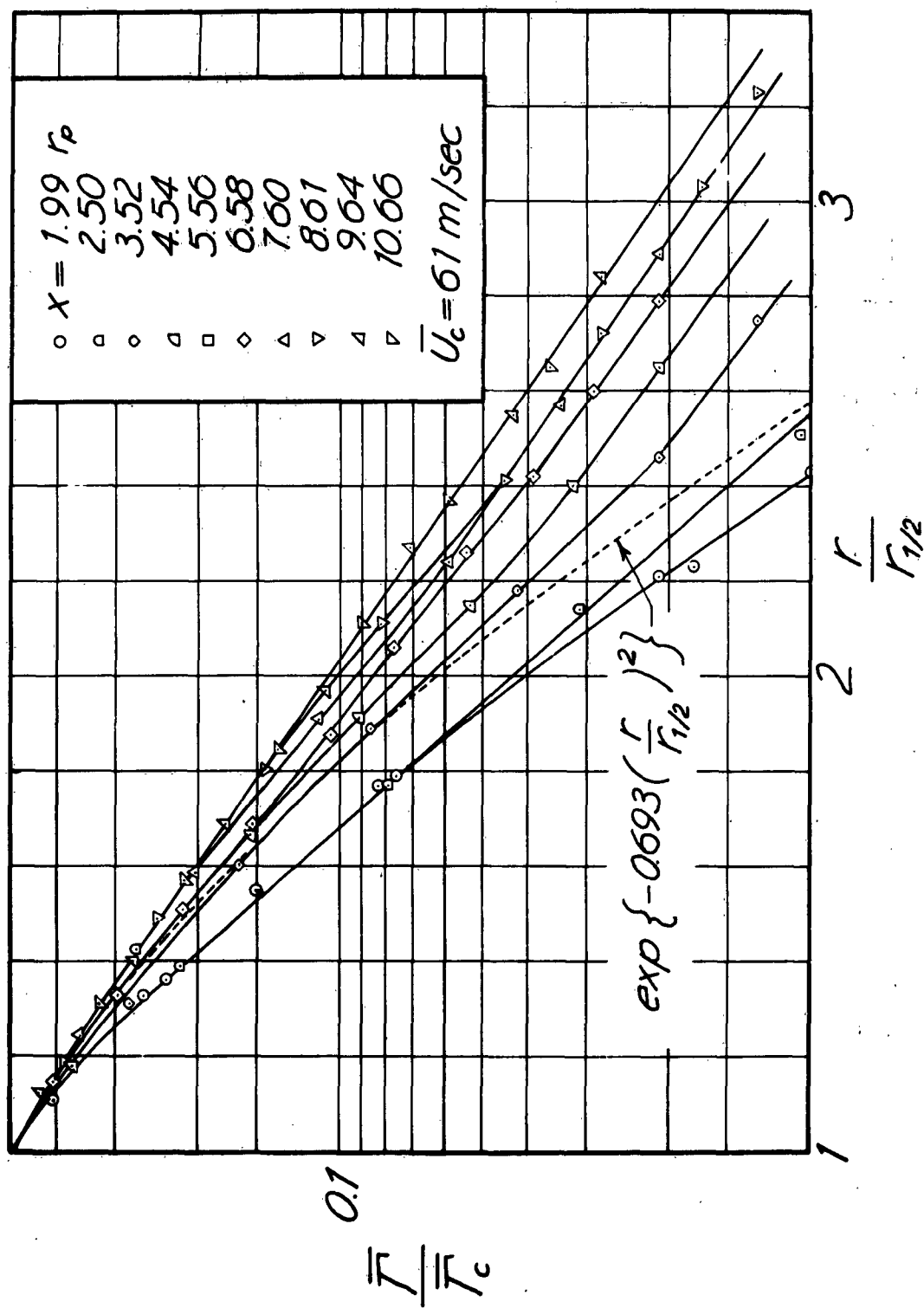


Figure 5: NORMALIZED RADIAL PROFILES OF THE POINT CONCENTRATION

self-preservation would have been closely approached far downstream of the source.

It should be remembered that the present profiles were obtained by moving the source across a pipe diameter while holding the point of observation fixed on the axis. Hence the radius r here measures distance from the center of the resulting profile, not from the axis of the pipe. Had the mean velocity been radially uniform and the turbulence fully homogeneous and isotropic, there would have been no difference between this and the converse mode of traversing. In the actual experiment, there should be no practical difference up to at least $r = r_p/2$: The maximum value of the plume half-radius $r_{1/2}$ in Figures 4 and 5 is approximately $1/4$ of a pipe radius. Within this distance from the center of a pipe flow at a pipe Reynolds number of 700,000, the mean velocity does not change by more than 3% of the centerline value, nor do the turbulence properties affecting diffusion vary significantly. Hence turbulent diffusion at $r < r_p/2$ was, in effect, affected only by the centerline mean velocity \bar{U}_0 and the centerline turbulence properties. The absence of a tendency toward self-preservation at the skirts of the concentration profile at large distances from the source can be attributed largely to the increasing penetration, as the pipe wall is approached, of regions exhibiting pronounced radial variation of the mean velocity and of the turbulence properties affecting diffusion.

The mean-square material displacement from the plume centerline is

$$\bar{r^2} = \frac{\int_0^\infty r^2 \bar{F} d(\pi r^2)}{\int_0^\infty \bar{F} d(\pi r^2)}$$

For the normal distribution (Equation 1), $\bar{r^2}$ is related to the half-radius $r_{1/2}$ by the proportionality

$$\bar{r}^2 = r_{1/2}^2 / 0.693. \quad (2)$$

Equation 2 applies, to a fair approximation, to the present data; the departures from the normal distribution occurring at the fringes of the diffusion plume cannot easily be held account of and, for large distances from the source, are properly ignored if interest is restricted to the core region of the pipe flow in which the mean velocity was essentially constant and the turbulence nearly homogeneous and isotropic. With use of Equation 2, the parameters in Taylor's statistical theory of one-particle diffusion are easily evaluated. The theory gives for one component of mean-square material displacement the relations

$$\bar{y}^2 = \bar{v}^2 t^2 \quad (3)$$

for small diffusion times and

$$\bar{y}^2 = 2 \bar{v}^2 T_L (t - t_0) \quad (4)$$

for large diffusion times, where v is the y -component of fluctuation in the particle velocity, T_L is the integral time-scale of the particle motion (called the Lagrangian time-scale), and t_0 is the virtual temporal origin of the final period of diffusion. For an axisymmetrical diffusion plume, v is the radial component of particle velocity and $\bar{y}^2 = 1/2 \bar{r}^2$. For a turbulence field translated past the diffusion source at high velocity (i.e., $\bar{U} \gg v$, fully realized in the core of a pipe flow), $t = x / \bar{U}$. The Lagrangian integral time scale T_L can be expressed in terms of the Lagrangian integral length scale Λ_L as $T_L = \Lambda_L / v$. With these substitutions, Equations 3 and 4 give for the present case

$$r_{1/2}^2 = 2(0.693) \bar{v}^2 x^2 / \bar{U}^2 \quad (5)$$

for the neighborhood of the source and

$$r_{1/2}^2 = 4(0.693) \hat{v} \Lambda_L (x - x_0) / \bar{U}_0 \quad (6)$$

for the domain far downstream. Here $\hat{v} \Lambda_L (= \bar{v}^2 T_L)$ is identical with the turbulent material diffusivity \mathcal{D}_T .

Figure 6 shows $r_{1/2}/r_p$ as a function of x/r_p for the neighborhood of the source. The linearity predicted by Equation 3 is not demonstrated, owing to the absence of data very near the source (a closer approach to the source was not practical with the present apparatus; a micrometer screw would have been needed to accurately position the fog injector. In any case, data for the region very near the source would have been of dubious significance, owing to the finite initial size of the plume and to the disturbance of the equilibrium pipe flow by the fog injector). A tangent to the experimental data, produced from the origin (assuming the effective origin to be coincident with the source) should, it appears, have a slope closely approximating $\sqrt{1.386} \hat{v} / \bar{U}_0$. The relative intensity of the radial fluctuation in the velocity of a diffusing particle is thus estimated to be $\hat{v} / \bar{U}_0 = 0.0284$. Baldwin and Walsh (1) studied diffusion of heat from a line source in airflow through a 20 cm (8 inch) nominal diameter commercial pipe 45 diameters long at mean velocities of 22, 32, 41, and 49 m/sec and estimated values of \hat{v} / \bar{U}_0 of 0.027, 0.029, 0.028, and 0.032. The agreement with the present result is very close and is certainly within the probable experimental error.

Figure 7 shows $r_{1/2}^2/r_p^2$ as a function of x/r_p . The linearity predicted by Equation 6 for the far downstream regime is very well realized. The spatial origin of the final period lies 1.95 pipe diameters downstream of the source. From the slope, 0.0065, it is estimated that $\hat{v} \Lambda_L / \bar{U}_0 r_p = 0.00235$. On substituting the value 0.0284 for \hat{v} / \bar{U}_0 , this gives for the Lagrangian spatial scale $\Lambda_L = 0.083 r_p$. Since $\hat{v} \Lambda_L$ is the turbulent material diffusivity, we have for the turbulent Peclet

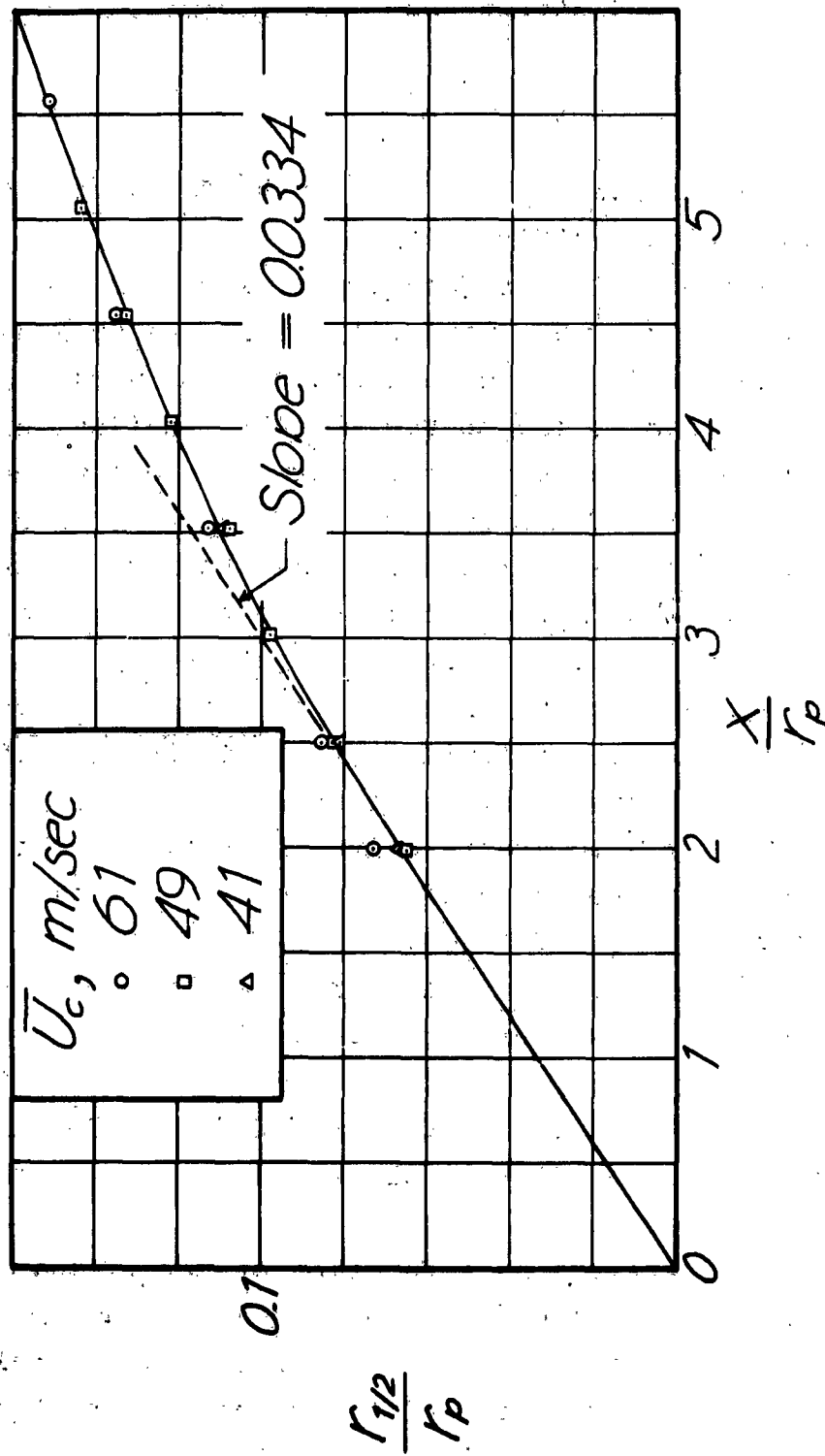


Figure 6: THE CONCENTRATION HALF-RADIUS OF THE PLUME AS A FUNCTION OF DISTANCE FROM THE SOURCE

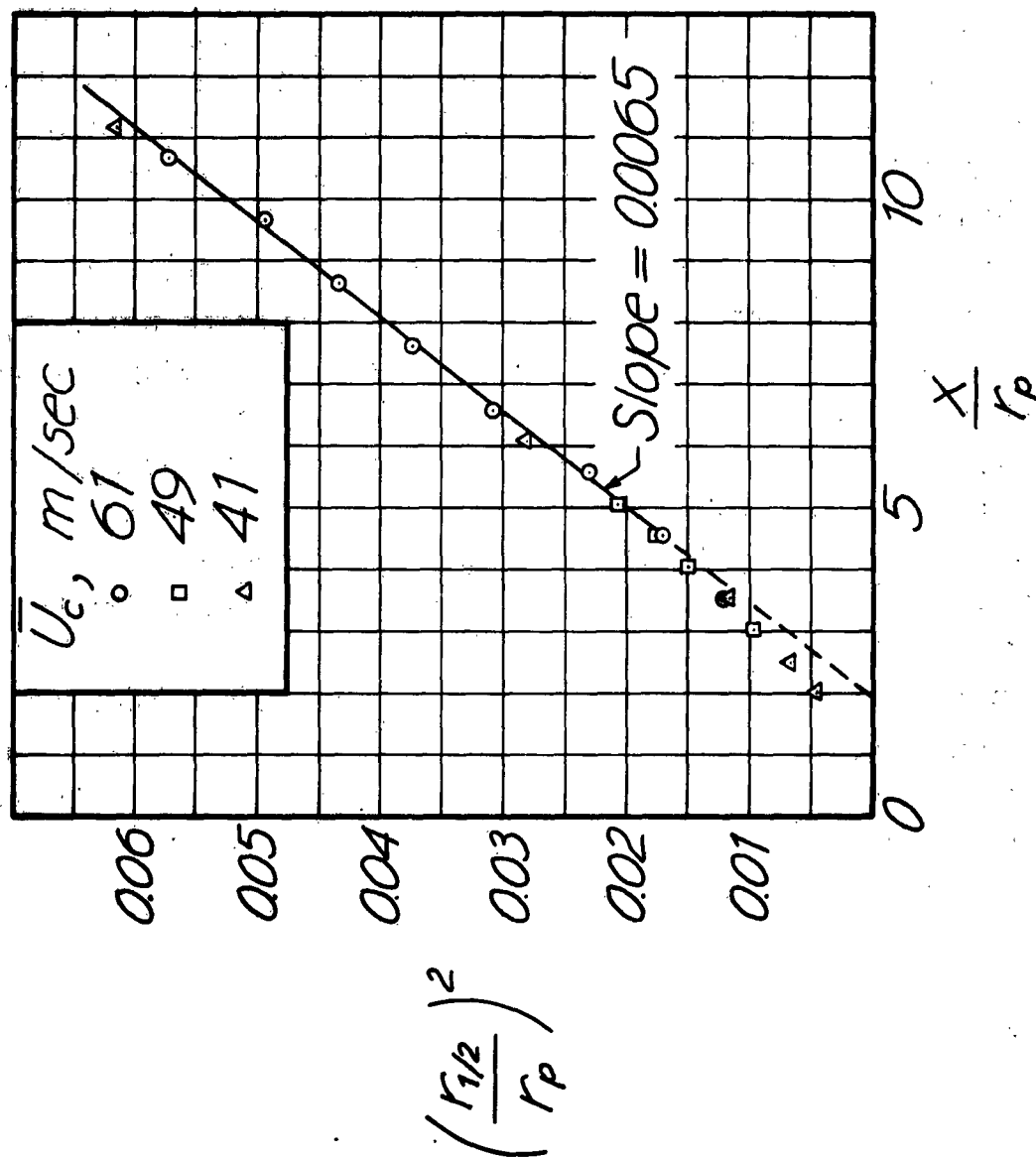


Figure 7: THE SQUARE OF THE CONCENTRATION HALF-RADIUS AS A FUNCTION OF DISTANCE FROM THE SOURCE

number the value $Pe_T (\equiv D_p \bar{U}_0 / \mathcal{D}_T) = 2/0.00235 = 852$. Baldwin and Walsh (1) obtained an average value of 910. Towle and Sherwood's data (22) on material diffusion in air indicate $Pe_T \approx 850$ at high Reynolds numbers. The data of Flint (8) on air and Kada (8) on water, however, indicate a value of 1250. Mickelson's data (16) on air scatter between 800 and 1200. The present data were obtained with less disturbance of the pipe flow by both the material source and the detection device than in any previous work (the optical probe indeed caused no disturbance whatever). Hence the present value of $Pe_T = 850$ can probably be regarded as definitive. It should be noted that the present data pertain to the case of a diffusing material (submicron-size oil droplets) with a negligible "molecular" diffusivity. In the case of hydrogen in air, molecular diffusion is quite significant, and Flint (8) calculated turbulent diffusivities from his data by assuming that turbulent and molecular diffusion are additive processes motivated alike by the mean concentration gradient.

The turbulent material diffusivity is constant, according to Taylor's theory (21), only in the final period of diffusion when the instantaneous and the initial particle motions are no longer correlated in any significant degree. A solution of the classical gradient diffusion equations for a constant diffusivity and constant mean velocity gives for the present case (10)

$$\bar{\Gamma} = \frac{J}{4\pi \mathcal{D}_T \sqrt{x^2 + r^2}} \exp \left\{ - \frac{U_0 (\sqrt{x^2 + r^2} - x)}{2 \mathcal{D}_T} \right\}, \quad (7)$$

where J is the source strength. Near the x -axis, $r \ll x$ and $\sqrt{x^2 + r^2} = x(1 + r^2/x^2)^{1/2} \approx x + 1/2 r^2/x$, giving

$$\bar{\Gamma} \approx (J/4\pi \mathcal{D}_T x) \exp \left\{ - U_0 r^2 / 4 \mathcal{D}_T x \right\}; \quad (8)$$

On the axis,

$$\bar{F} = \bar{F}_0 = J/4\pi \mathcal{D}_T x. \quad (9)$$

The radial concentration distribution near the axis can therefore be written

$$\bar{F} \sim \bar{F}_0 \exp \left\{ - U_0 r^2 / 4 \mathcal{D}_T x \right\} \quad (10)$$

Comparison with Equation 1 then gives

$$r_{1/2}^2 = 4(0.693) \mathcal{D}_T x / \bar{U}_0. \quad (11)$$

On locating the origin of x at the virtual origin, x_0 , of the final diffusion period, this relation is seen to be identical with that (Equation 6) obtained from Taylor's theory. In accord with the present experimental results, the gradient diffusion model predicts that the radial concentration distribution near the plume axis will take the form of the normal distribution.

In the case of a radially-constant mean velocity, the material flux through any cross-section of the diffusion plume is

$$\bar{U}_0 \int_0^\infty \bar{F} d(\pi r^2) = J. \quad (12)$$

It is therefore expected for the present case that the product $\bar{F}_0 r_{1/2}^2$ should be essentially constant. Table 2 confirms this expectation.

TABLE 2
CONSTANCY OF THE PRODUCT $\bar{F}_0 r_{1/2}^2$ AT $Re_p = 684,000$

x/r_p	1.99	3.01	3.52	4.53	5.56	6.58	7.60	8.61	9.64	10.7
$\bar{F}_0/r_{1/2}^2$	1.03	1.03	1.00*	0.98	0.99	1.05	0.98	0.97	0.95	1.01

*Reference value

The Spectrum of Point-concentration Fluctuations

The mean-square concentration fluctuation at a point can be decomposed into contributions from different frequencies. We have thus the relation

$$\overline{\gamma^2} = \int_0^{\infty} E_{\gamma_1}(k_1) dk_1, \quad (13)$$

where $E_{\gamma_1}(k_1)$ is the one-dimensional wave-number spectral density function and $k_1 \equiv 2\pi f / \bar{U}$ is the wave number.

Spectral analyses were carried out at a pipe Reynolds number of 450,000 for points on the plume axis 2, 7, and 11 pipe radii from the source. The volume optically probed by the scattered-light technique was of necessity rather large, approximately 1.5 mm in diameter, and due corrections (5) were made to obtain the true point-concentration fluctuation spectrum. At high wave numbers, the information content of the signal was obliterated by the shot noise associated with the photocathode current (Schottky's schroteffekt). The shot noise level could have been lowered by increasing the signal strength; in effect, by observing a larger volume or by using a stronger material source. Increasing the observed volume, however, would have attenuated the high wave-number content of the signal very seriously. The source strength could have been increased by using a larger-diameter fog injector, but a larger injector would have very seriously disturbed the pipe flow. In sum, the present sizes of light probe and fog injector were in the optimum range decreed by opposing limitations on effective operation. Consequently no really significant improvement of performance was possible, if we reject as possibilities such things as the development of a markedly better fog or the becoming available of a considerably intenser light source.

Figure 8 shows the spectra obtained. The trend toward simplification of spectrum shape with increasing distance from the source might be expected on the grounds of a tendency towards equilibrium. The $(-5/3)$ -power variation of spectral density with wave number expected at high wave numbers for an equilibrium

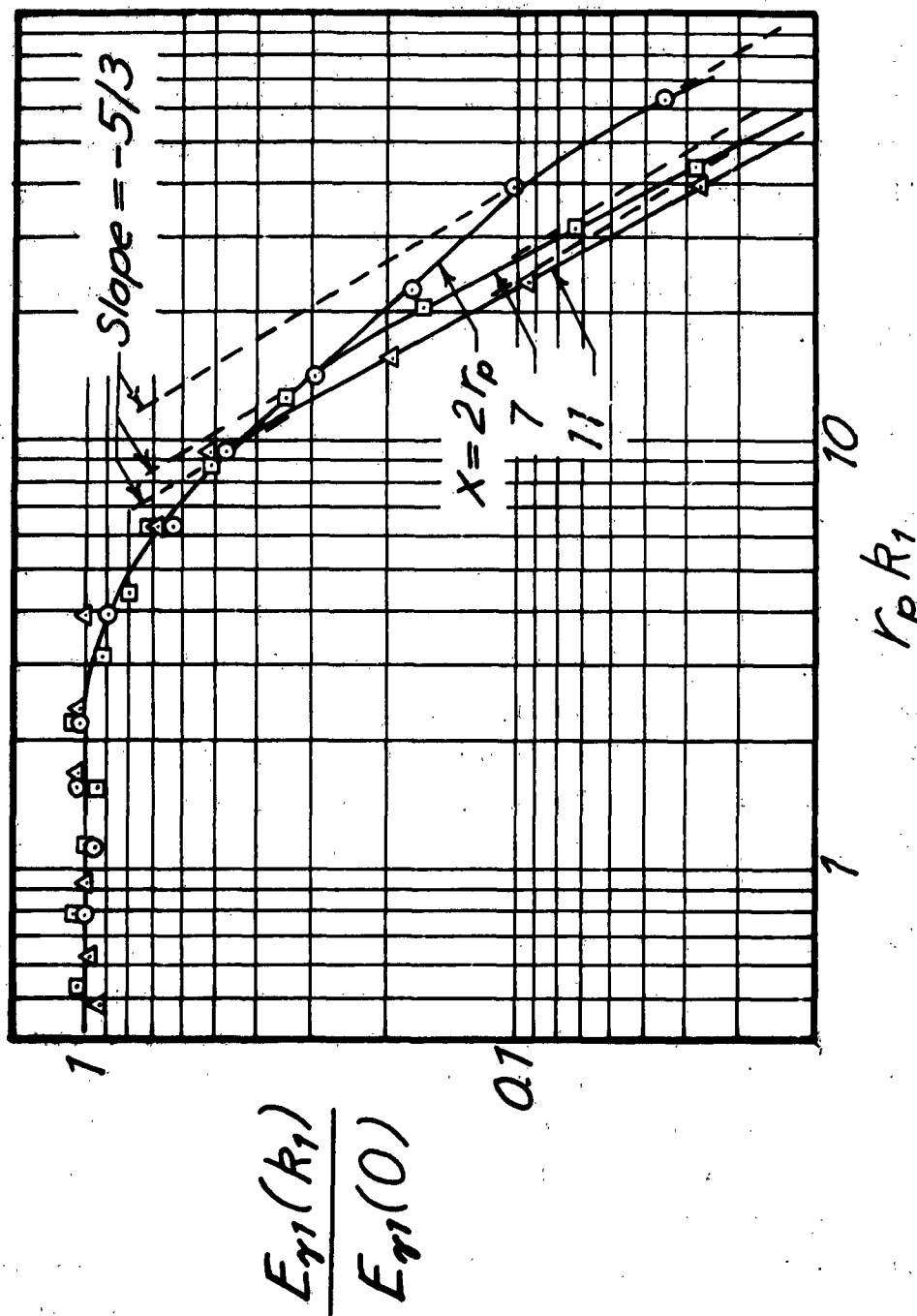


Figure 8: NORMALIZED ONE-DIMENSIONAL SPECTRA OF POINT CONCENTRATION FLUCTUATIONS

convection subregime is approximated, but the data do not really extend to high enough wave numbers to warrant a conclusion. The trend in the configurations of the spectra is opposite to that found by Lee and Brodsky (14) for the diffusion of dye in water, but the significance of this difference is uncertain. Their injector (0.6 cm in diameter by 130 cm long and installed on the axis of a 7.5 cm diameter pipe) quite considerably disturbed the pipe flow in their experiment. Their optical probe was nearly three times larger in relative diameter than the present (1 mm in a 75 mm pipe) and had elements which physically entered the flow, disturbing the point of observation.

From the intercept at zero wave-number, the integral spatial scale of the concentration fluctuations can be estimated:

$$\Lambda_Y = (\pi/2) E_{Y1}(k_1=0) / \overline{\gamma^2}. \quad (14)$$

The scales calculated are $\Lambda_Y = 0.081 r_p$ at $x = 2r_p$; $0.10 r_p$ at $7 r_p$, and $0.11 r_p$ at $11 r_p$. These values are of similar magnitude with that found for the Lagrangian scale, $\Lambda_L = 0.084 r_p$.

It should be noted that the values quoted for Λ_Y are about appropriate to the case of a molecular Schmidt number, $\mu/\rho D_M$, of approximately unity (realized physically in the case of gas mixing): In using Equation 13 for the calculation of $E_{Y1}(0)/\overline{\gamma^2}$, the spectral density function was assumed to follow a $-5/3$ power law at high wave numbers. A material such as oilfog has, however, an exceedingly high "molecular Schmidt number, i.e., the fog particles diffuse Brownianly with the extremest sloth. In this case the spectrum is expected to exhibit a very broad (-1) -power region at high wave numbers (2), leading to very much higher values of $\overline{\gamma^2}$ and very much lower values of Λ_Y than those presently found. The disregard seen here for the actual system under study need occasion no alarm. It is much more interesting, for most practical applications in chemical engineering and meteorology, to extract the consequences the data have for gas mixing than to worry about what ultimately happens in the rather

academic case of an arbitrarily near-infinite Schmidt number. The very high wave-number end of the oilfog-diffusion spectrum is, of course, experimentally inaccessible, for the material eddies small enough to be affected by Brownian diffusion are microscopic in size. In relation to mixing in liquids, it would be interesting to penetrate the high wave-number end sufficiently to fix the beginning of the (-1) -power regime. A much smaller lightprobe than was practicable for the present work would be needed, however.

The Intensity of Point-concentration Fluctuations

The r.m.s. (root-mean-square) amplitude of a turbulent fluctuation is commonly referred to as the intensity of that fluctuation. A complete mapping was made of the intensity of concentration fluctuations in the diffusion plume. As already implied in the discussion of the spectrum, the use of a rather large light probe caused a cutoff in response at fairly low wave numbers, in consequence of which the measured intensities give a picture of gas, not oilfog, diffusion; i.e., the case of a molecular Schmidt number on the order of unity is portrayed.

Figure 9 exhibits the intensity data in the form of the normalized profile

$$\hat{\gamma} = F_0 \cdot h(r/r_{1/2}),$$

where $r_{1/2}$ is the mean-concentration half-radius. The profiles appear to be self-preserving; there is no visible change with downstream position. There is, however, a surprising tendency for the intensity to decrease with increasing Reynolds number (the centerline velocity of 61 m/sec corresponds to a Reynolds number of 684,000).

Figures 10 and 11 exhibit the data with the intensity expressed as a fraction of the local mean concentration,

$$\hat{\gamma} = F_0 \cdot j(r/r_{1/2}),$$

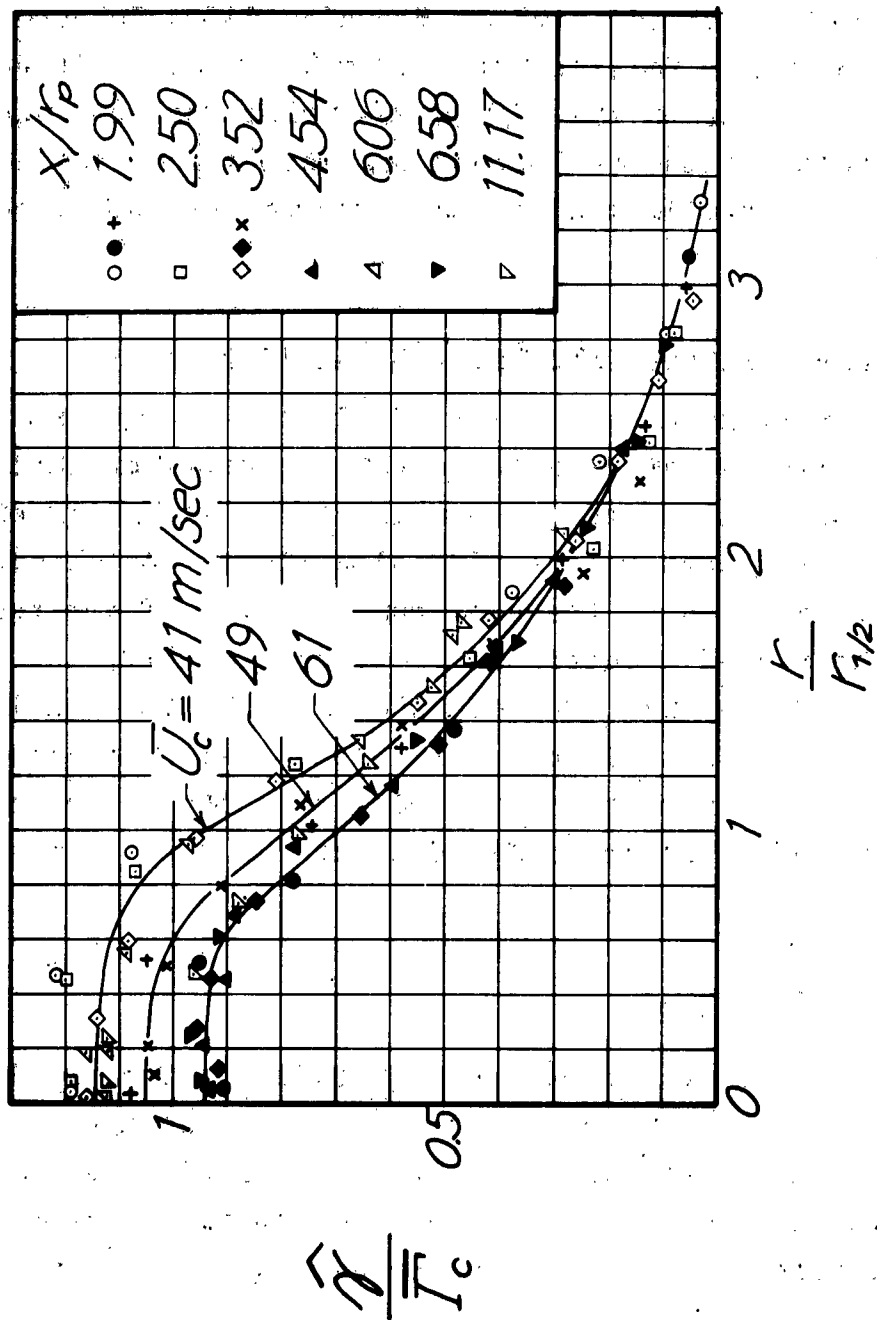


Figure 9: NORMALIZED RADIAL PROFILES OF THE INTENSITY OF POINT CONCENTRATION FLUCTUATIONS

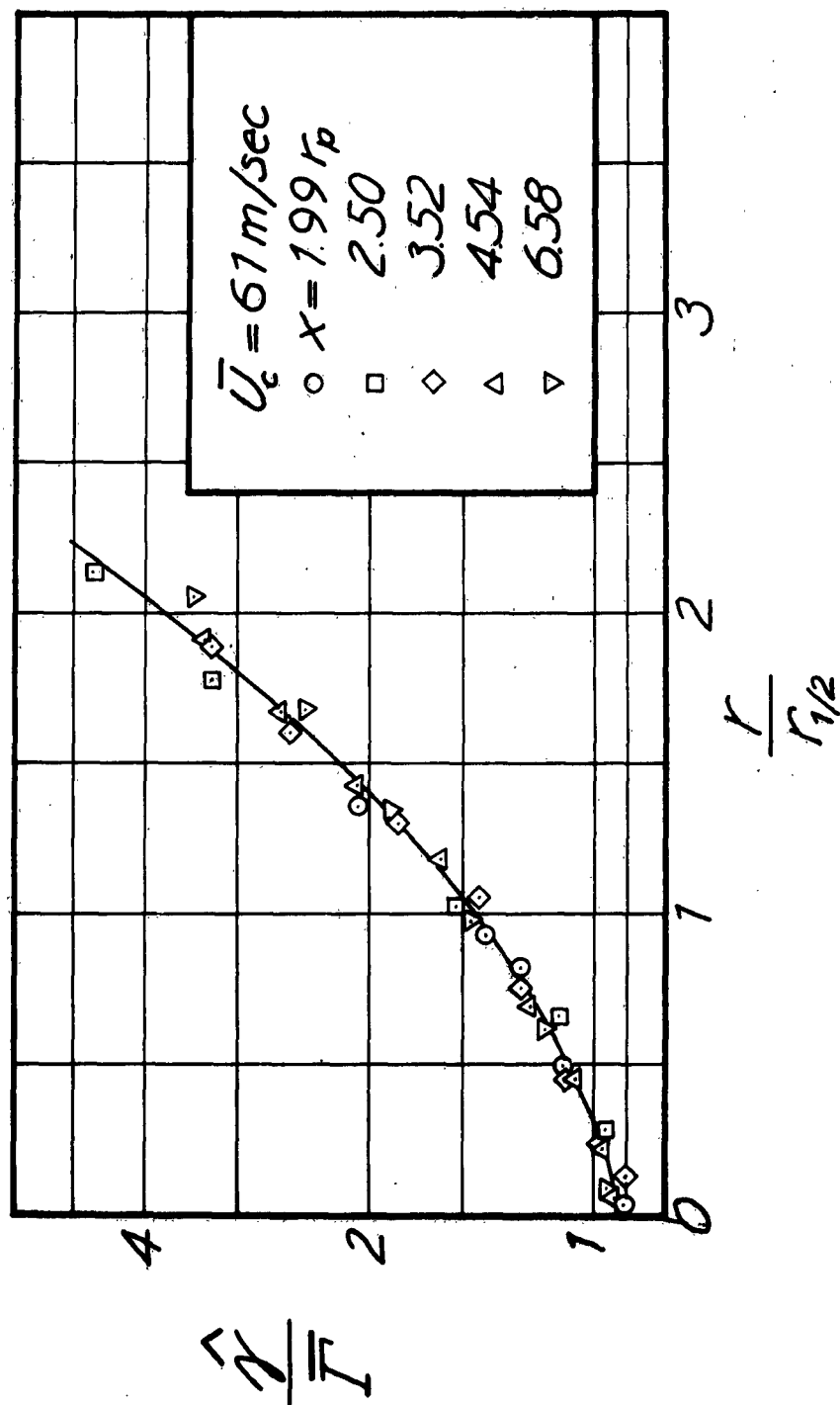


Figure 10: NORMALIZED RADIAL PROFILES OF THE RELATIVE INTENSITY OF POINT-CONCENTRATION FLUCTUATIONS

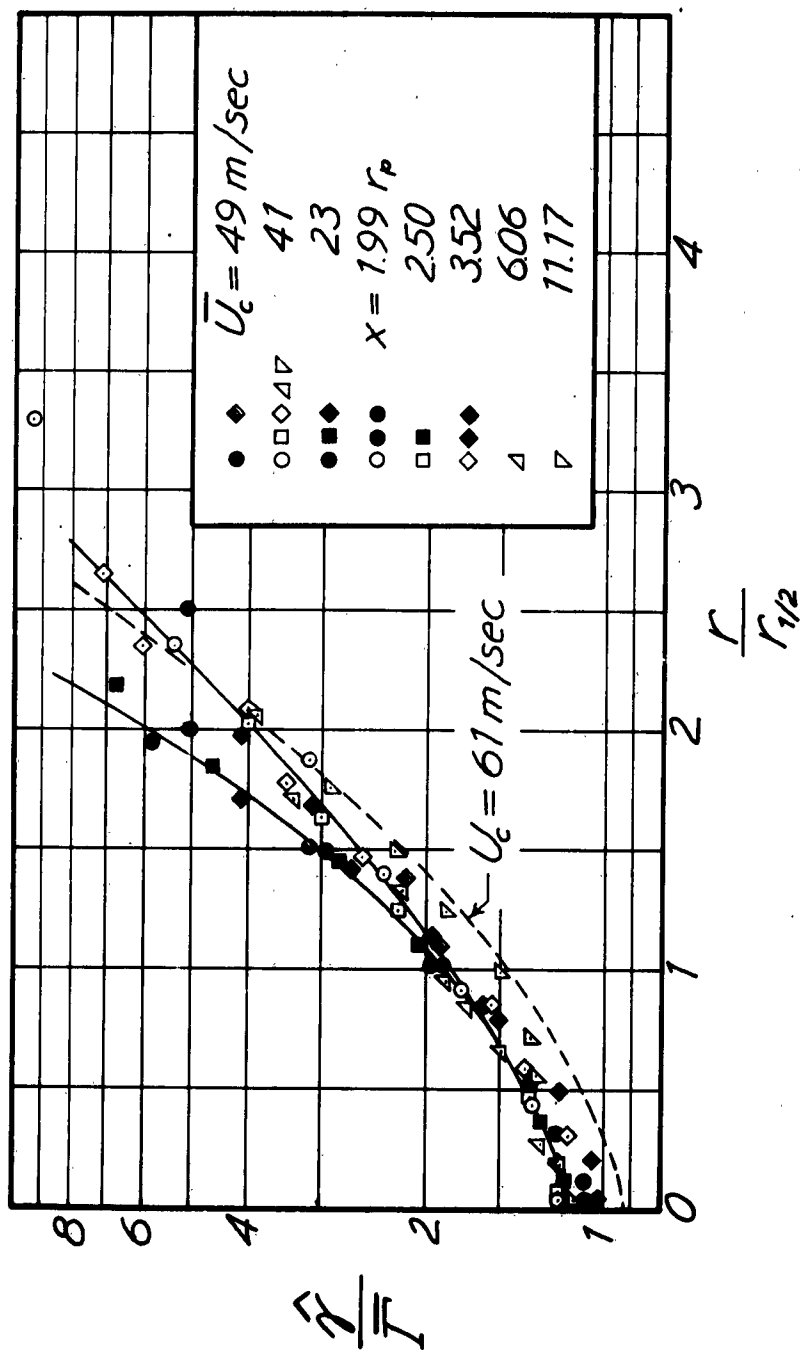


Figure 11: NORM.LIZED RADIAL PROFILES OF THE RELATIVE INTENSITY OF POINT-CONCENTRATION FLUCTUATIONS

a ratio usually spoken of as the relative intensity of fluctuation. It is seen that the relative intensity, already very high on the plume axis, increased rapidly with radial distance. The value of approximately unity on the axis may be compared with the value of about 0.25 attained in turbulent jets (3).

The shapes of the profiles seen in Figure 9 are quite similar to those obtained by Lee and Brodsky (14) for the diffusion of dye in water. The fluctuation amplitudes they observed are, however, only 1/6 as high. This disparity seems greater than can be accounted for by any proper difference between the two systems. The sources of error possible for the present measurements would appear to lead to underestimation of the intensity, not vice versa. It would seem, therefore, that Lee and Brodsky's results should be verified before any firm comparison of gas and liquid systems is ventured.

The Intensity of Sheet-concentration Fluctuations

The term "sheet-concentration" is meant to facilitate reference to the quantity

$$\Omega \equiv \int_0^{2\pi} \int_0^{\infty} \Gamma \cdot r \cdot dr \cdot d\phi \quad (15)$$

Since $\Omega \cdot dx$ is the quantity of material in a sheet of thickness dx , Ω is the material density in one dimension of space, a type of one-dimensional concentration.

The time-mean and fluctuating components of Ω are

$$\bar{\Omega} = \int_0^{\infty} \bar{\Gamma} d(\pi r^2) \quad (16)$$

and

$$\omega \equiv \int_0^{2\pi} \int_0^{\infty} \gamma \cdot r \cdot dr \cdot d\phi. \quad (17)$$

The mean-square value of the sheet-concentration fluctuations depends on the two-point spatial correlation of the point-concentration fluctuations. To develop this relation very simply, write

for ω

$$\omega \equiv \int_A \gamma \, dA, \quad (18)$$

where dA is an area element in the domain, A , of material presence in the plume cross-section of interest. Then

$$\overline{\omega^2} = \overline{\left(\int_A \gamma \, dA \right)^2} = \int_A \int_A \overline{\gamma' \gamma} \, dA' \, dA, \quad (19)$$

where $\overline{\gamma' \gamma}$ is the correlation between the concentration fluctuations occurring in the area elements dA and dA' . This correlation can be expressed as the product of the point-concentration fluctuation intensities multiplied by a correlation coefficient $C(x, r, \phi, r', \phi')$ giving

$$\overline{\omega^2} = \int_A \int_A \hat{\gamma}' \hat{\gamma} C \, dA' \, dA. \quad (20)$$

The simplest behaviour possible for the correlation coefficient C is a dependence solely on the distance, ζ , between the area elements dA and dA' ; $C = C(\zeta)$. The simplest form probable for $C(\zeta)$ is $C(\zeta) = \exp(-\zeta/\Lambda_\gamma)$, where Λ_γ is the integral scale of the material eddies,

$$\Lambda_\gamma = \int_0^\infty C(\zeta) \, d\zeta. \quad (21)$$

It is evident from Equation 20 that, owing to the area-weighting of C , the sheet-concentration intensity will depend largely on the behavior of C at separation distances larger than Λ_γ . In other words, the value of ω , will as one should intuitively expect, be affected most by the large-scale material eddies. Thus the use of sheet illumination in the scattered-light technique affords a means of emphasizing the properties of the large-scale eddies, facilitating the study of these in considerable isolation. The elucidation of large-eddy properties will be elaborated in a subsequent paper; the present will simply record the data obtained to date.

Figure 12 shows the relative intensity of sheet-concentration fluctuations in the diffusion plume as a function of distance from the source. The relative intensity increases at a decreasing rate with downstream distance, tending (as should be expected) toward an equilibrium value. There is a surprisingly large dependence on the meanflow velocity and the direction of change is opposite to that exhibited by the point-concentrations (see Figure 9). Because of the oddness of this result, the data were carefully verified. It would appear from the trends exhibited that the point-concentration fluctuations at large separation distances were more highly correlated at the higher flow velocity.

The Spectrum of Sheet-concentration Fluctuations

The sheet-concentration fluctuations, like the point-concentration fluctuations, can be spectrally analyzed and the mean-square fluctuation decomposed into contributions from different frequencies or wave numbers:

$$\overline{w^2} = \int_0^{\infty} W(k_1) dk_1, \quad (22)$$

where $W(k_1)$ is the spectral density function and $k_1 \equiv 2\pi f / \bar{U}_0$ is the wave number. Since Ω and ω are one-dimensional concepts to begin with, there is no problem (as in the case of point-concentration fluctuations) with one-dimensional (i.e., line) sampling of a three-dimensional space. Thus $W(k_1)$ should reflect quite directly the distribution of the material eddies associated with ω . In particular, there should appear to be few eddies of very large diameter and so the wave-number spectrum should be distinctly hump-like in shape.

The sheet-concentration fluctuations were spectrally analyzed at several downstream distances and flow velocities. Figures 13 and 14 confirm the general expectation as to the spectrum shape. The significance of the low-level plateau apparent in Figure 14 at very low wave numbers is uncertain. Figures 14, 15, and 16 show that the spectra tended toward a

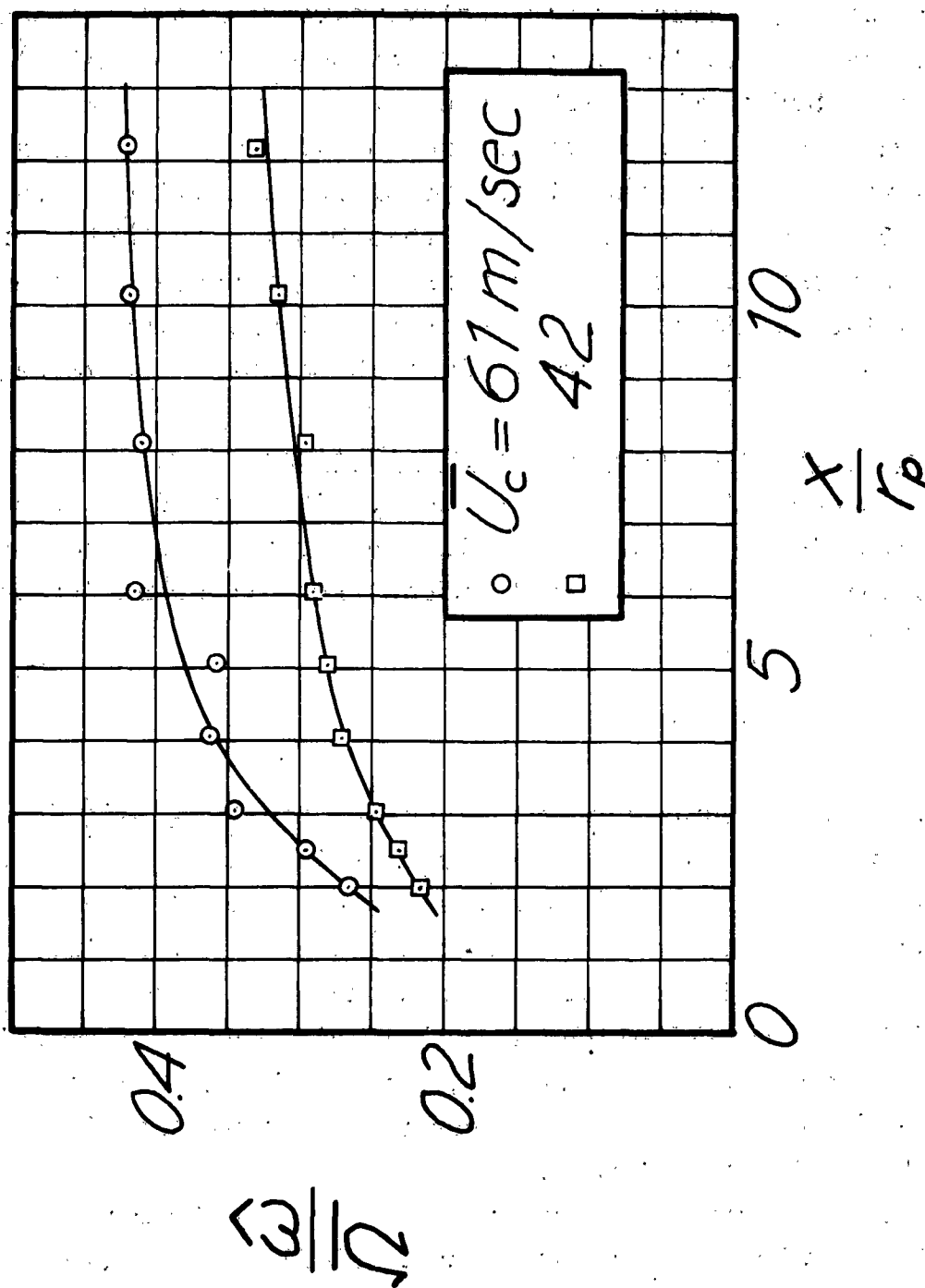


Figure 12: THE NORMALIZED INTENSITY OF SHEET-CONCENTRATION FLUCTUATIONS AS A FUNCTION OF DISTANCE FROM THE SOURCE

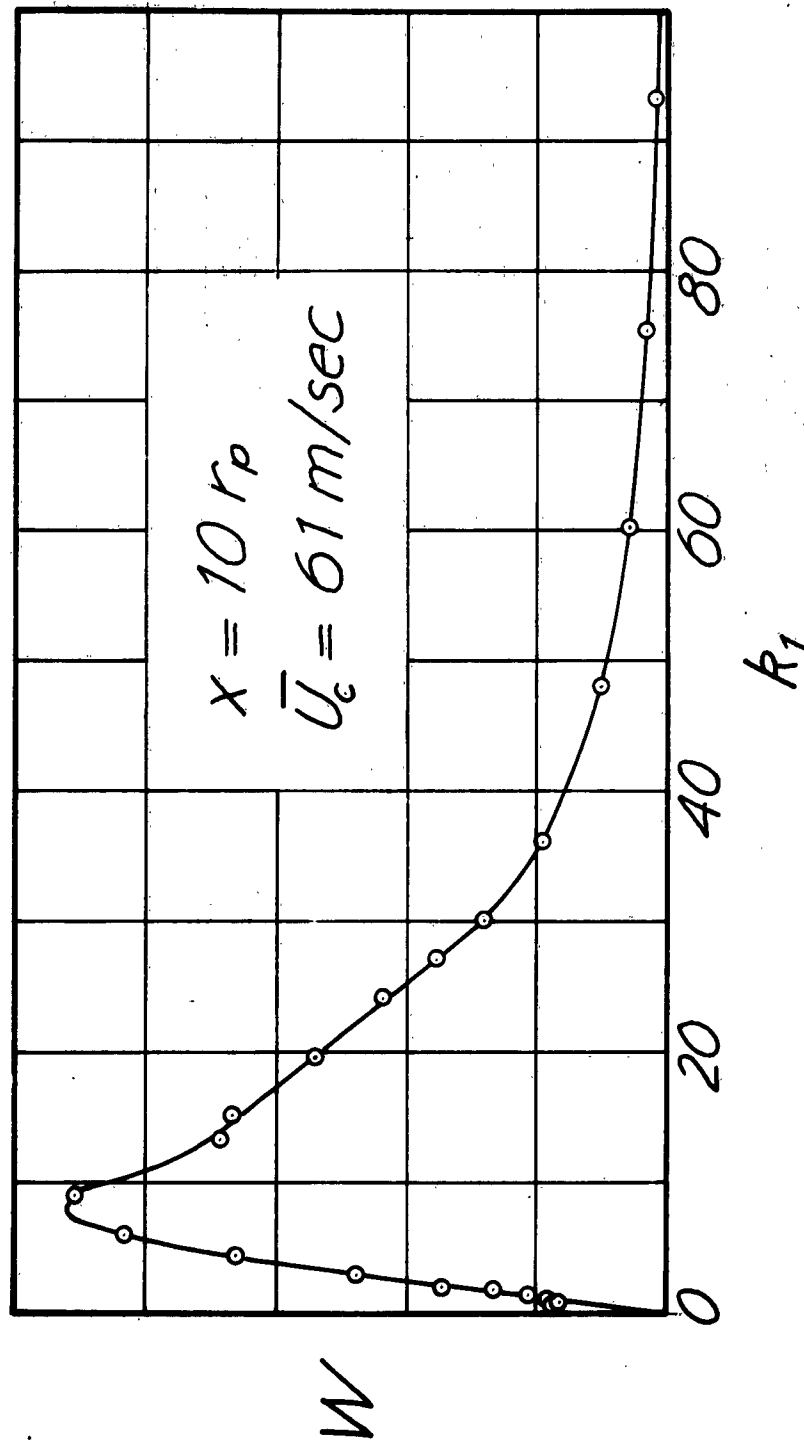


Figure 13: A REPRESENTATIVE SPECTRUM OF SHEET-CONCENTRATION FLUCTUATIONS

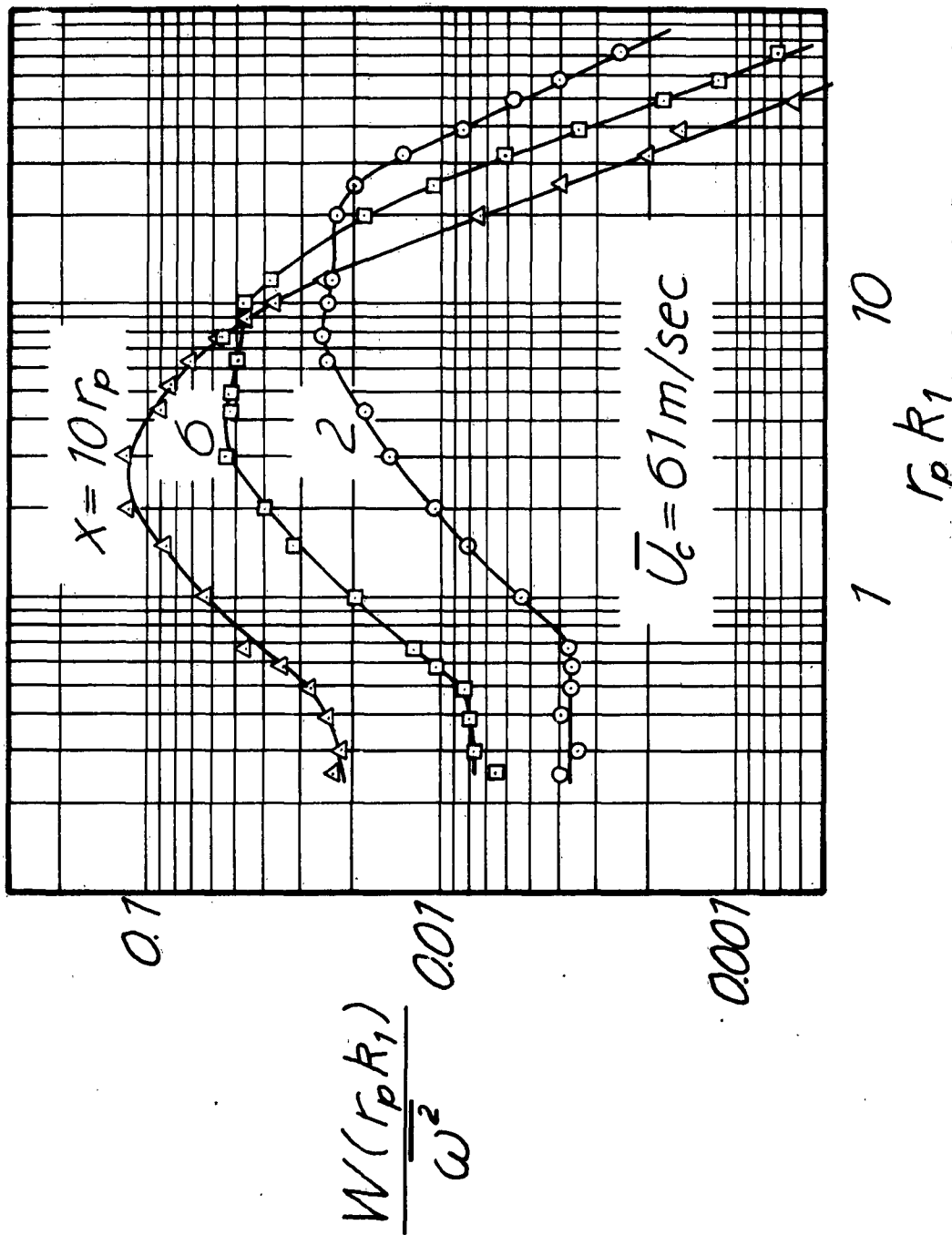


Figure 14: SPECTRA OF SHEET-CONCENTRATION FLUCTUATIONS AT VARIOUS DISTANCES FROM THE SOURCE

simple limiting form at sections far from the source - a featureless hump, nearly symmetrical in a log-log representation. Near the source variations in mean velocity produced considerable change, Figure 15, but the effect diminished with downstream distance, Figure 16. The differences between the spectra in Figure 16 are within the experimental error.

In order to afford a clear comparison of the spectral shapes for the limiting regime far from the source, the data in Figure 16 are shown in the normalized form

$$W = \bar{w} W(k_1 / k_{1/2}), \quad (23)$$

where $k_{1/2}$ is the centroid of the spectrum:

$$\bar{w}/2 = \int_0^{k_{1/2}} W(k_1) dk_1. \quad (24)$$

Now the reciprocal of the wave number is identified with eddy size; hence $(k_{1/2})^{-1}$ is an average measure of the spatial scale of the eddies affecting most the value of \bar{w} . Figure 17 shows the dependence of this scale on distance from the source. The irregularity of the data probably has little general significance: Firstly, the possible error in estimating $k_{1/2}$ was fairly large, and secondly, a somewhat erratic behaviour is not altogether unexpected for the large eddies dominating the composition of \bar{w} . All that can be conclusively said is that $(k_{1/2})^{-1}$ is of similar magnitude with the plume half-radius (compare Figures 6 and 17).

The reciprocal, k_m^{-1} , of the wave number at which the maximum of the spectral density function occurs is another measure of average eddy size, more poorly defined than $(k_{1/2})^{-1}$. This scale is shown as a function of downstream distance in Figure 18.

The spectrum of sheet-concentration fluctuations is most easily interpreted in terms of the corresponding correlation function obtained from it by Fourier transform. The correlation

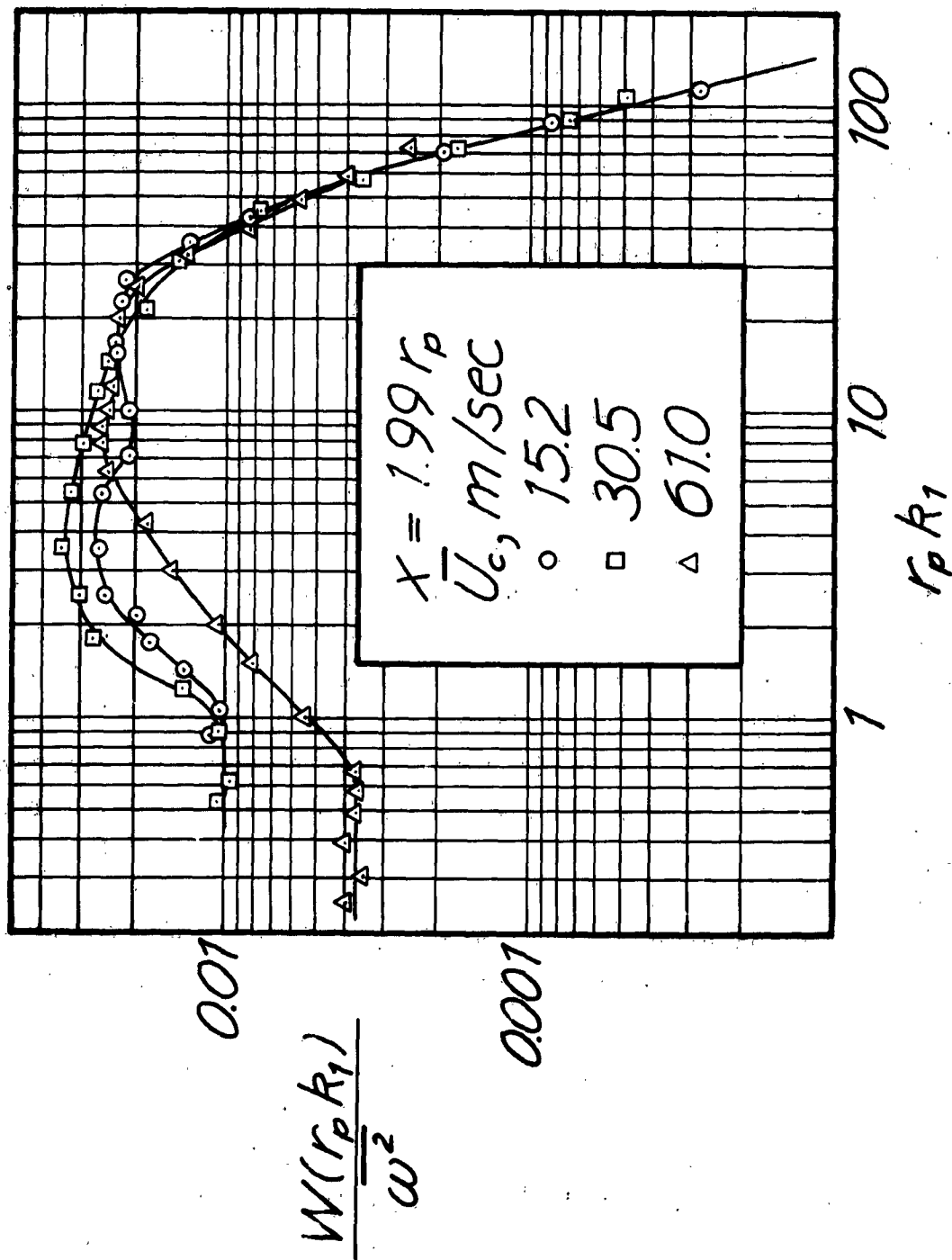


Figure 15: SPECTRA OF SHEET-CONCENTRATION FLUCTUATIONS NEAR THE SOURCE AT VARIOUS FLOW VELOCITIES

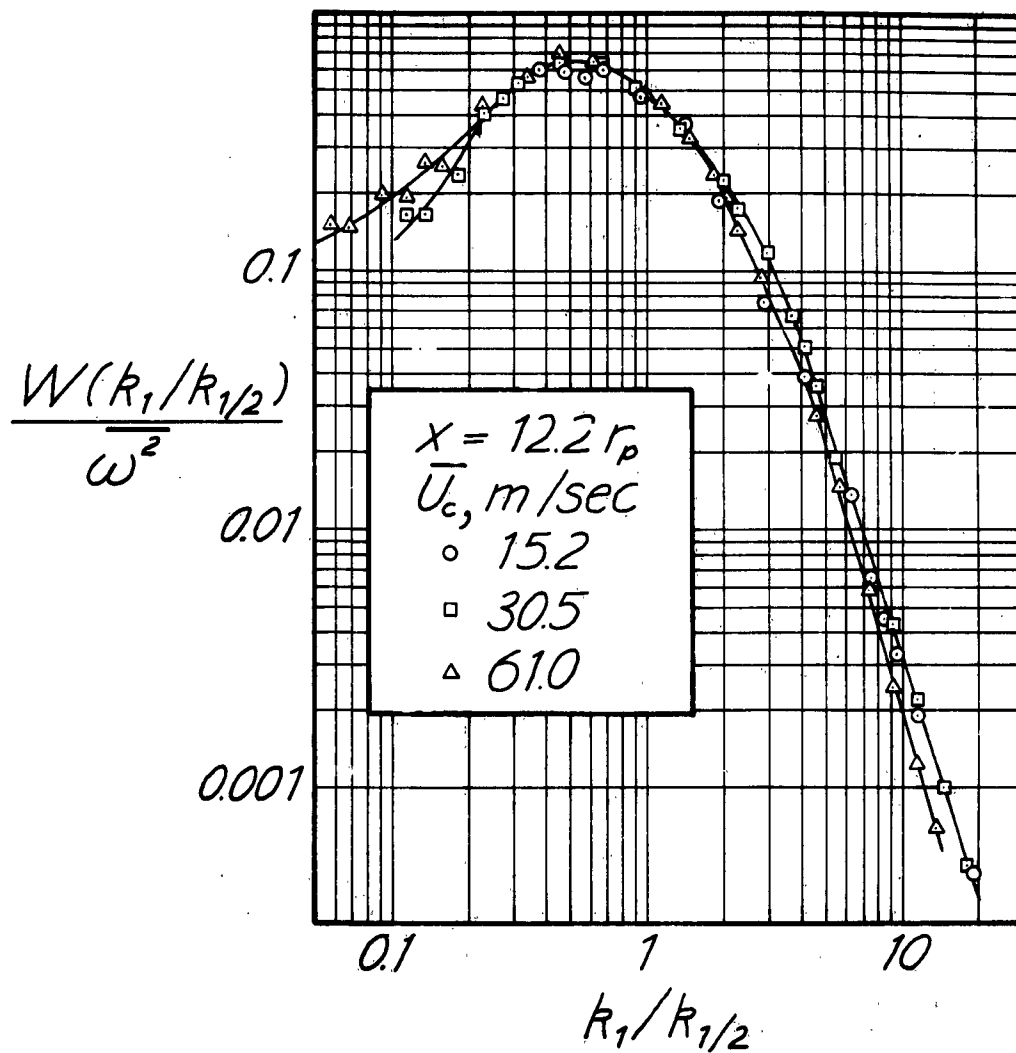


Figure 16: SPECTRA OF SHEET-CONCENTRATION FLUCTUATIONS FAR FROM THE SOURCE AT VARIOUS FLOW VELOCITIES

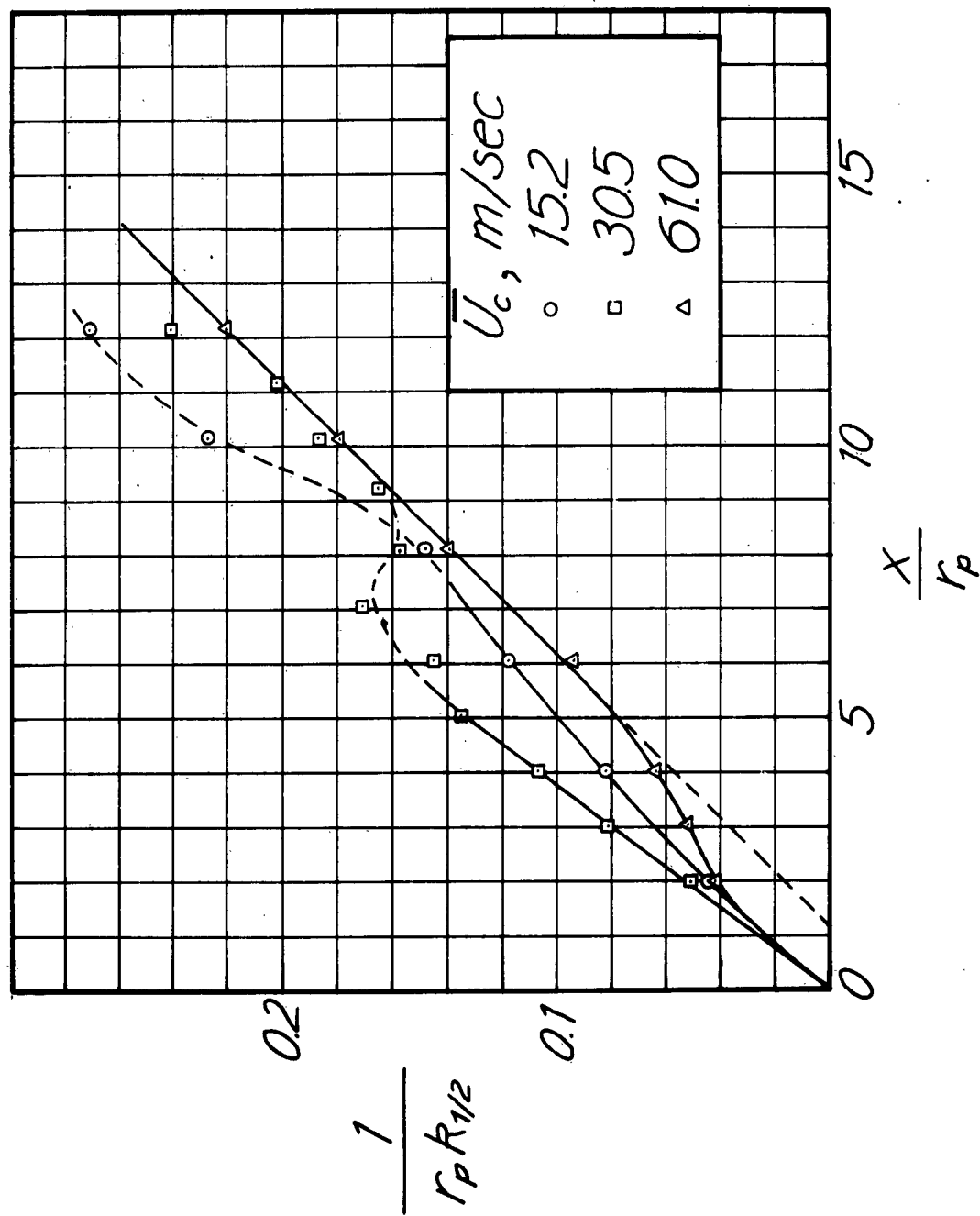


Figure 17: RELATION BETWEEN THE CENTROID OF THE SPECTRUM OF SHEET-CONCENTRATION FLUCTUATIONS AND DISTANCE FROM THE SOURCE

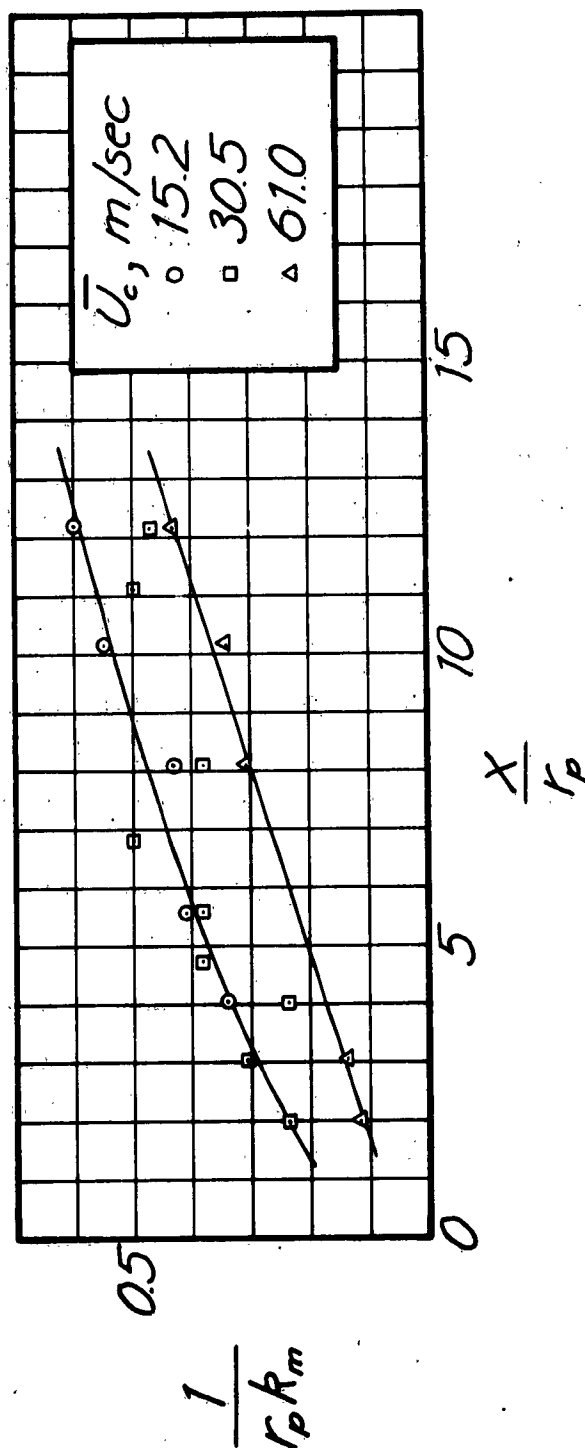


Figure 18: RELATION BETWEEN THE MAXIMUM-POINT OF THE SPECTRUM OF SHEET CONCENTRATION FLUCTUATIONS AND DISTANCE FROM THE SOURCE

in question is

$$\overline{\omega' \omega} \equiv \overline{\omega(x') \omega(x)}.$$

In terms of point-concentration fluctuations,

$$\overline{\omega' \omega} = \overline{\int_A \gamma \, dA \int_{A'} \gamma' \, dA'} = \int_A \int_{A'} \overline{\gamma' \gamma} \, dA' \, dA, \quad (25)$$

where the cross-sections A and A' cut the diffusion plume at x and x' and $\overline{\gamma' \gamma}$ is the correlation between point-concentration fluctuations in the area elements dA' and dA. This correlation can be expressed in terms of a correlation coefficient and the local point-concentration fluctuation intensities, giving

$$\overline{\omega' \omega} = \int_A \int_{A'} \hat{\gamma}' \hat{\gamma} C(x, r, \rho, x', r', \rho') \, dA' \, dA. \quad (26)$$

In the simplest case, C depends only on the distance of separation, ζ , between dA and dA'. The correlation function $\overline{\omega' \omega}$ can itself be expressed in terms of a correlation coefficient K:

$$\overline{\omega' \omega} = \hat{\omega}' \hat{\omega} K(x, x') = \hat{\omega}(x) \hat{\omega}(x+\eta) K(x, \eta),$$

where $\eta \equiv x' - x$.

The computation of correlations from the present spectra has been begun, but final results are not yet available. The spectrum and correlation functions discussed by Laurence (13) suggest that K has approximately the form

$$K = (1 - \eta/\Lambda_w) \exp(-\eta/\Lambda_w),$$

where Λ_w is a measure of the spatial scale of the sheet-concentration fluctuations. This correlation coefficient is negative at large separation distances, having a minimum value of -0.135 at $\eta = 2\Lambda_w$.

Meandering

A method was devised for using the scattered-light technique,

with sheet illumination, to detect meandering; in particular, to measure the mean-square displacement of the instantaneous center of gravity from the time-mean center of a plume cross-section. The method utilizes two phototransducers on opposite sides of the plume at equal distances L from the axis and simultaneously viewing edge-on the uniformly illuminated cross-section. The amount of scattered light received by a phototube from an area element dA is proportional directly to the point-concentration, Γ , in dA and inversely to the square, q^2 , of the distance between dA and the viewing lens. Thus the total instantaneous signal developed by the phototube is

$$E = S \int_A \frac{\Gamma}{q^2} dA, \quad (27)$$

where S is the overall sensitivity. Suppose now that the viewing lens is far enough from the plume so that the cosine of one-half the angle through which the plume is seen is essentially unity. Let L be the distance from the lens to the plume axis and let the y -coordinate be parallel to the line of sight on the axis, as shown in Figure 19. The signal E can then be expressed as

$$E = S \int_A \frac{\Gamma}{(L+y)^2} dA. \quad (28)$$

In the case that $y \ll L$ within the domain of non-zero Γ ,

$$\begin{aligned} E &\approx \frac{S}{L^2} \int_A \Gamma \left(1 - 2 \frac{y}{L}\right) dA \\ &\approx \frac{S}{L^2} \left(\int_A \Gamma dA - \frac{2}{L} \int_A y \Gamma dA \right) \\ &\approx \frac{S}{L^2} \left(1 - 2 \frac{Y_0}{L} \right), \end{aligned} \quad (29)$$

where Y_0 is the instantaneous center of gravity. If this is the signal produced by a phototube on one side of the plume, then that simultaneously produced on the other side must be

$$E' = S' \int \frac{\Gamma}{A (L-y)^2} dA, \quad (30)$$

and in the limit $y \ll L$

$$E' = \frac{S}{L^2} (1 + 2 Y_0/L). \quad (31)$$

The mean-square fluctuating signal produced by either phototube at large viewing distances L is easily shown to be proportional to $\overline{\omega^2} + 4 \overline{\Omega^2} \overline{Y_0^2}/L^2$, while the mean signal is simply proportional to $\overline{\Omega}$. Thus the ratio, P , between the mean-square fluctuation and the square of the mean is

$$P = \overline{\omega^2} / \overline{\Omega^2} + 4 \overline{Y_0^2} / L^2. \quad (32)$$

Consider now the correlation between the fluctuating signals from the two phototubes; at large L

$$\overline{e'e} = \frac{S'S}{L^2} \overline{\Omega^2} (\overline{\omega^2} / \overline{\Omega^2} - 4 \overline{Y_0^2} / L^2). \quad (33)$$

Dividing by $e'e$, there is obtained the correlation coefficient

$$Q = \frac{1 - 4(\overline{\Omega^2} / \overline{\omega^2})(\overline{Y_0^2} / L^2)}{1 + 4(\overline{\Omega^2} / \overline{\omega^2})(\overline{Y_0^2} / L^2)} \quad (34)$$

Note that the value of Q depends on two processes: The fluctuations in Ω sensed by two phototransducers are perfectly positively correlated, (i.e., always of the same sign) having therefore a correlation coefficient of +1. The displacements Y_0 in the instantaneous center of gravity sensed by the two transducers are, on the other hand, perfectly negatively correlated, (i.e., always of opposite sign) and have therefore a correlation coefficient of -1. Thus the value of the overall correlation coefficient Q lies between +1 and -1 and depends on the relative amplitudes of the two

fluctuation processes. The relative amplitude of the meander process can be controlled by adjusting the viewing distance, L . One must not, however, in attempting to emphasize that process, make L so small as to invalidate the linearization of the transducer response.

Provision was made for mounting a phototransducer downstream of and practically at right-angles to the illuminated plume cross-section, i.e., in a position insensitive to meandering. The ratio between the mean-square fluctuation and the square of the mean for the signal developed here is simply $\overline{w^2}/\overline{L^2}$. Thus, by measuring the relative intensity of the sheet-concentration fluctuations with this transducer and either P or Q with the transducers at the sides of the plume, the mean-square meander $\overline{Y_0^2}$ can be calculated from Equation 32 or Equation 34. Since the effect of meandering was expected to be small (owing to the large values of L necessary for the linearization of response) and since Q is about twice as sensitive to meandering as P, present efforts were concentrated on measuring the correlation coefficient Q. The measurements were expedited by a correlation amplifier, the output of which was impressed on the r.m.s. voltmeter and developed the value of the correlation coefficient directly on a special scale on the voltmeter.

The value of the viewing distance L in the experiments was 20 cm, and a significantly smaller value could not be used (except in the region very near the source) without invalidating the assumption of linear response. With this value of L , the observed correlation coefficients were insignificantly smaller than +1. Thus, while no quantitative data were obtained, it was established that meandering is a small effect in the final period of diffusion.

To put this result in proper perspective, suppose that \hat{Y}_0 was 1/2 cm at $r_{1/2} = 2$ cm (a plume radius appropriate to $x = 10 r_p$). Then, with $L = 20$ cm, $\overline{Y_0^2}/L^2 = (1/40)^2$. According to Figure 12, an appropriate value of $\overline{L^2}/\overline{Y_0^2}$ is 10. Then $Q = (1 - 4(10)/(40)^2)/(1 + 4(10)/(40)^2) = 0.951$. It therefore

appears that, in the final diffusion period at least, Y_0 is of the order of $1/2$ or smaller than $1/4 r_{1/2}$.

The meandering process should be much more pronounced in the initial period of diffusion, i.e., in the domain near the source. At the small plume diameters occurring near the source, a smaller significantly viewing distance L than 20 cm should have been used. However, the present phototransducers could not be deployed so near the plume axis without seriously disturbing the flow. Since there was insufficient time remaining, finally, for building the necessary miniaturized transducers, the detection of meandering was not pursued further,

DISCUSSION

The mean-square material displacement, $\overline{Y^2}$, from the instantaneous center of gravity is related to the mean-square displacement, $\overline{Y_0^2}$, of the instantaneous center of gravity from the time-mean center by the identity

$$\overline{y^2} \equiv \overline{Y^2} + \overline{Y_0^2}. \quad (35)$$

Thus knowledge of $\overline{y^2}$ and $\overline{Y_0^2}$ is sufficient to determine $\overline{Y^2}$. This $\overline{Y^2}$, as noted in the Introduction, is the basic quantity in Richardson diffusion. In Lin's formulation (15), Richardson's law gives for the present system

$$\overline{Y^2} = 1/3 Et^3 = 1/3 Bx^3 / \overline{U_0}^3 \quad (36)$$

The parameter B in this equation is, however, of most general interest because of its apparent relationship with Kolmogoroff's energy dissipation parameter ϵ .

The direct evaluation of $\overline{Y^2}$ by photographic means (the only reasonable method for our experimental system) was, as noted earlier, impossible with the resources of time and skilled personnel available for this investigation. The indirect approach,

via $\overline{Y_0^2}$ and $\overline{y^2}$, foundered on the measurement of $\overline{Y_0^2}$ near the plume source. However, the possibilities of the technique employed have not been exhausted and should be further examined (the use of miniaturized phototransducers allowing a close approach to the pipe axis without seriously disturbing the flow is indicated).

While the stated objects of the investigation - verification of Richardson's law and evaluation of Lin's parameter B - were not achieved, a rich yield of novel and useful information on other aspects of turbulent diffusion was obtained, especially respecting concentration fluctuations. The data on sheet-concentration fluctuations are quite unique and promise to be highly informative with regard to large-eddy structure.

The present results definitely indicate that meandering is a weak effect in the final period of dispersion in a pipeflow; none could be detected. The fluctuating-plume model of Gifford (9) is therefore invalid here, for very strong meandering indeed is needed to make this the principle source of concentration fluctuations. The condition for strong meandering may be more nearly realized in atmospheric turbulence, since the turbulence spectrum there is more favorable for this mode of dispersion.

One of the predictions of Gifford's theory was indeed confirmed; the relative point-concentration fluctuation γ/\overline{F} exhibited a minimum on the plume axis and increased monotonously toward the edges. This, however, is not of itself evidence for the theory. For example, it may be supposed that, to a first approximation, the material eddies in any plume cross-section are characterized by a uniform concentration Γ_E . The mean-square concentration fluctuation $\overline{\gamma^2}$ is then related to the mean concentration \overline{F} by the formula

$$\overline{\gamma^2}/\overline{F^2} = \Gamma_E/\overline{F} - 1.$$

For the usual bell-shaped \overline{F} profile, this equation also predicts a minimum for γ on the plume axis and a monotonous

increase towards the edges. When the present data are plotted in the form $\bar{\gamma}^2 / \bar{\Gamma}^2 + 1$ vs. $1 / \bar{\Gamma}$, an essentially linear relation is seen with a slope (identifiable with Γ_E) of $1.25 \bar{\Gamma}_c$.

The results of the present investigation have considerable practical significance. In problems occurring in the field, it is often not the mean but the instantaneous concentration of material in a diffusion plume that is of interest, e.g., is the concentration level of a gas, a vapor, a smoke, a fog, or a dust above a critical level? The present data facilitate the estimation of relevant statistical properties of the instantaneous concentration: Assuming point-concentration fluctuations are normally distributed, the probability density of fluctuations of amplitude γ is

$$(\gamma \sqrt{2\pi})^{-1} \exp \left\{ -\gamma^2 / 2\bar{\gamma}^2 \right\}$$

(near the source, the truncation of the distribution at the source concentration must, however, be considered). Since $\bar{\gamma}^2$ and $\bar{\Gamma}$ are given by the present data, we can now calculate, e.g., the probability $P(\Gamma > \Gamma')$ that the instantaneous concentration $\Gamma = \bar{\Gamma} + \gamma$ will exceed a threshold value Γ' . This probability is identical with the fraction of time over which the instantaneous concentration exceeds the threshold value. Thus we could examine, e.g., the possibility of finding breathable air in a plume of contaminant.

A similar use can be made of the data on sheet concentrations. One can estimate, for example, the fraction of time over which a line of sight across a field is obscured by an intervening plume of fog or smoke.

REFERENCES

1. Baldwin, L.V., and Walsh, T.J. A.I.Ch.E. Journal 7, 53 (1961)
2. Batchelor, G.K. J. Fluid Mech. 5, 113 (1959)
3. Becker, H.A. "Concentration Fluctuations in a Ducted Turbulent Jet". Sc.D. Thesis, Department of Chemical Engineering, M.I.T. (1961)
4. Becker, H.A., Hottel, H.C., and Williams, G.C. "Mixing and Flow in a Ducted Turbulent Jet". Ninth Symposium (International) on Combustion (1962)
5. Becker, H.A., Hottel, H.C., and Williams, G.C. "Characterization of Concentration Fluctuations in a Turbulent Jet by the Scattered-light Technique". A.I.Ch.E. Journal (1964)
6. Brier, G.W. J. Meteorology 7, 283 (1950)
7. Corrsin, S., and Uberoi, M.S. N.A.C.A. Report No. 1040 (1954)
8. Flint, D.L., Kada, H., and Hanratty, T.J. A.I.Ch.E. Journal 6, 325 (1960)
9. Gifford, F. "Advances in Geophysics", Vol. 6, Academic Press, New York (1959)
10. Hinze, J.O. "Turbulence". McGraw-Hill Book Co. Inc., New York (1959)
11. Hutchings, J.W. J. Meteorology 12, 263 (1955)
12. Lauffer, J. N.A.C.A. Report No. 1174 (1954)
13. Laurence, J.C. N.A.C.A. Report No. 1292 (1956)
14. Lee, J.L., and Brodsky, R.S. "Turbulent Motion and Mixing in a Pipe". Preprint No. 14, A.I.Ch.E. Symposium on mixing theory and experiment, held at Chicago (December, 1962)
15. Lin, C.C. Proc. Nat. Acad. Sci. 46, 566 and 1147 (1960)
16. Mickelson, W.R. N.A.C.A. TN 3570 (1955)
17. Richardson, L.F. Proc. Royal Soc. (London) Series A 110, 709 (1926)
18. Rosensweig, R.E. "Measurement and Characterization of Turbulent Mixing". Sc.D. Thesis, Department of Chemical Engineering, M.I.T. (1959)
19. Rosensweig, R.E., Hottel, H.C., and Williams, G.C. Chem. Eng. Sci. 15, 111 (1961)
20. Stommel, H. J. Marine Res. 8, 199 (1949)
21. Taylor, G.I. Proc. London Math. Soc. 20, 196 (1921)
22. Towle, W.L., and Sherwood, T.K. Ind. Eng. Chem. 31, 457 (1939)

<p>AF Cambridge Laboratories, Bedford, Mass., Rpt. No. AFRL-63-727. TURBULENT DISPERSION IN A PIPE FLOW. Final Report. October 63. 52 p. incl. illus., tables and 22 refs.</p> <p>Turbulent diffusion from a point source in a pipe flow has been studied. It was desired to verify Richardson's law and to evaluate the parameter B in Lin's derivation of that law. Difficulties were encountered and the data obtained were insufficient for these purposes. A very considerable quantity of novel and useful information was nevertheless gathered. The scattered-light technique was used to map the fields of point-concentration fluctuations and of the mean concentration in the diffusion plume. The relative intensity of the point-concentration fluctuations was found to be of the order of 100% on the plume axis and increased towards the plume edges. The parameters in Taylor's theory were evaluated; the intensity of fluctuations in the radial component of the velocity of a diffusing particle was estimated to be 2.84% of the centerline velocity in the pipe, and the Lagrangian (spatial) integral scale was found to be of the</p>	<ol style="list-style-type: none"> 1. Turbulent diffusion 2. Concentration fluctuations 3. Scattered-light technique 4. Pipe flow <ol style="list-style-type: none"> I. Project No. 8604 Task No. 86040 II. Contract AF19(604)-6181 III. Fuels Research Laboratory, Massachusetts Inst. of Technology, Cambridge, Mass. IV. H.A. Becker, et al. V. In DUC collection 	<p>AF Cambridge Laboratories, Bedford, Mass., Rpt. No. AFRL-63-727. TURBULENT DISPERSION IN A PIPE FLOW. Final Report. October 63. 52 p. incl. illus., tables and 22 refs.</p> <p>Turbulent diffusion from a point source in a pipe flow has been studied. It was desired to verify Richardson's law and to evaluate the parameter B in Lin's derivation of that law. Difficulties were encountered and the data obtained were insufficient for these purposes. A very considerable quantity of novel and useful information was nevertheless gathered. The scattered-light technique was used to map the fields of point-concentration fluctuations and of the mean concentration in the diffusion plume. The relative intensity of the point-concentration fluctuations was found to be of the order of 100% on the plume axis and increased towards the plume edges. The parameters in Taylor's theory were evaluated; the intensity of fluctuations in the radial component of the velocity of a diffusing particle was estimated to be 2.84% of the centerline velocity in the pipe, and the Lagrangian (spatial) integral scale was found to be of the</p>	<ol style="list-style-type: none"> 1. Turbulent diffusion 2. Concentration fluctuations 3. Scattered-light technique 4. Pipe flow <ol style="list-style-type: none"> I. Project No. 8604 Task No. 86040 II. Contract AF19(604)-6181 III. Fuels Research Laboratory, Massachusetts Inst. of Technology, Cambridge, Mass. IV. H.A. Becker, et al. V. In DUC collection
<p>magnitude of 8.3% of the pipe radius. The value resulting for the turbulent Peclet number (the product of pipe diameter times centerline velocity divided by turbulent diffusivity) is 853. The use of sheet-illumination in the scattered-light technique facilitated the measurement of fluctuations in the integral concentration of material in a plume cross-section. The relative intensity of these fluctuations was of the order of 30%. Spectral analyses were made of both point- and sheet- concentration fluctuations and integral turbulence scales were estimated from the data.</p>		<p>magnitude of 8.3% of the pipe radius. The value resulting for the turbulent Peclet number (the product of pipe diameter times centerline velocity divided by turbulent diffusivity) is 853. The use of sheet-illumination in the scattered-light technique facilitated the measurement of fluctuations in the integral concentration of material in a plume cross-section. The relative intensity of these fluctuations was of the order of 30%. Spectral analyses were made of both point- and sheet- concentration fluctuations and integral turbulence scales were estimated from the data.</p>	